FINAL REPORT on

ADVANCED LOST FOAM CASTING TECHNOLOGY

Phase V

By

WANLIANG SUN

HARRY E. LITTLETON

And

CHARLES E. BATES

TO

THE DEPARTMENT OF ENERGY,

THE AMERICAN FOUNDRY SOCIETY,

and

AFS-DOE-LFC FOAM CASTING CONSORTIUM MEMBERS

DOE CONTRACT N0. DE-FC07-99ID13840

REPORT NO. 527985-2004 Project Final Report

February 2005

ADVANCED LOST FOAM CASTING TECHNOLOGY, PHASE V

Table of Contents

EXECUTIVE SUMMARY 5

ACCOMPLISHMENTS

1. Computational Model and Data Base 10

1.1 Pattern Material Degradation Properties Data Base 10
1.1.1 Characterization of Pattern Degradation through Foam Pyrolysis 10
    1.1.1.1 Heater Material 11
    1.1.1.2 Heater Size and Shape 11
    1.1.1.3 Gas Generation Regimes 13
    1.1.1.4 Gas Generation Rate 13
    1.1.1.5 Temperature of Gaseous and Liquid Pyrolysis Products 13
    1.1.1.6 Resistance Pressure of Pattern Degradation 14
    1.1.1.7 Molecular Weight of Foam Pyrolysis Products 14
    1.1.1.8 Effects of Molded and Sawed Surfaces 14
    1.1.1.9 Effects of Foam Pattern Fusion Level 14
    1.1.1.10 Degradation of Pattern Adhesives 15

1.1.2 Visualization of Metal Foam Replacement through Real Time X-Ray Technology 16
    1.1.2.1 Real Time X-Ray Apparatus 16
    1.1.2.2 Metal Filling of Lost Foam Aluminum Castings 18
        Experiment Matrix; Coating Perm and Pattern Fusion Level; Foam Density; Coating Permeability; Glue Joint; Metal Filling and Casting Quality; Damaged Coating; Sectional Metal Front Profile
    1.1.2.3 Interior Quality of Lost Foam Aluminum Castings 21
    1.1.2.4 Effects of Pattern Tooling Types on Metal Filling 21
    1.1.2.5 Metal Filling of Lost Foam Iron Castings 22

1.1.3 Pattern Degradation and Casting Defect Formation 23
    1.1.3.1 Effect of Down Sprue Design 23
    1.1.3.2 Effect of Process Parameters on Defect Formation 23
    1.1.3.3 Effect of Foam Materials (T180 and T185) 24
    1.1.3.4 Effect of Alloy Chemistry 25
    1.1.3.5 Effect of Superheat and Hydrogen Content 26
    1.1.3.6 Development of Defect Database 26

1.2 Computational Model 27
1.2.1 Problems of Existing Codes 27
1.2.2 Development of Physical Model 28
1.2.3 Development of Algorithms 29
1.2.4 Achievement in Computational Model 29
1.2.5 Validation and Improvement with Real Time X-Ray 31

2. Casting Dimensional Accuracy ········ 31

2.1 Identify Sources of Casting Distortion ········ 31

2.1.1 Case Study 1: Long Pipe ········ 31
2.1.2 Case Study 2: Valve Body ········ 31
2.1.3 Sources of Casting Distortion ········ 33

3. Pattern Production ········ 33

3.1 Pattern Bead Properties ········ 33
3.1.1 Properties of Raw Beads ········ 33
3.1.2 Pattern Density Measurement with Dielectric Sensors ········ 34
3.1.3 Pattern Permeability ········ 34
    3.1.3.1 Apparatus ········ 34
    3.1.3.2 Pattern thickness and fusion level ········ 34
    3.1.3.3 Pattern permeability, metal filling and casting quality ·· 36
    3.1.3.4 Threshold of air flow rate ········ 37
3.1.4 Computational modeling of Bead Filling and Steaming ········ 37

3.2 Pattern Tooling ········ 37
3.2.1 Tooling design ········ 37
3.2.2 Tooling Types ········ 38
3.2.3 Filling and Bead Arrangement ········ 38
3.2.4 Pattern Molding Parameters ········ 39
    3.2.4.1 Experimental approach ········ 39
    3.2.4.2 Pattern fusion level ········ 39
    3.2.4.3 Open porosity ········ 40
    3.2.4.4 Density Gradient ········ 40
    3.2.4.5 Foam pattern temperature and pressure ········ 41
3.2.5 Pattern Properties and Casting Quality ········ 41
3.2.6 Pattern Quality Control Manual ········ 42

4. Improved Pattern Materials and Processes ········ 42

4.1 Improved Pattern Materials ········ 42
4.1.1 Foam Pattern Pre-coat ········ 42
4.1.2 Development of "No Fold" Bead Materials ········ 43
4.1.3 Evaluation of Alternative Foam Materials – Polyurethane ········ 43
4.1.4 Evaluation of Alternative Foam Materials – PMMA ········ 44

4.2 Improved Pattern Degradation Process ········ 44
4.2.1 Pattern Additives ········ 44
4.2.2 Coating Additives ········ 45
4.2.3 Effects of Pouring Atmosphere ········ 45
4.2.4 Minimum Degradation Energy ········ 45

5 Coating Control ······································ 46

5.1 Coating Quality Control ································ 46
5.1.1 Coating Control – Case Study ························ 46
5.1.2 Correlation between UAB and GM Coating Permeability Test ····· 46
5.1.3 Reorientation of Research Focus ······················ 47

5.2 Coating Consistency ···································· 47

5.3 Vacuum Assist ·· 47
5.3.1 Drawback of Vacuum Assist ··························· 47
5.3.2 Metal Filling of Lost Foam Iron with Vacuum Assist ·········· 48

6. In-Plant Case Studies and Technology Exchange ··················· 48

6.1 Case Study – Equipment Maintenance ····························· 48
6.2 Case Study – Gas Cavity and Cold Laps in Lost Foam Iron Castings ······· 49
6.3 Case Study – Pattern Quality and Casting Quality ················ 50
6.4 Case Study – Pattern Permeability Control on the Production Floor ······· 50
6.5 Case Study - "House keeping" on the production Floor ··········· 50
6.6 Case study – Leakage in Cylinder Head ·························· 51

7. Energy and Environmental Data ·································· 51

8. Technology Transfer ··51

Acknowledgements ···53

Use of This Report and Information Contained Herein ·················54

ADVANCED LOST FOAM CASTING TECHNOLOGY

EXECUTIVE SUMMARY

Previous research, conducted under DOE Contracts #DE-FC07-89ID12869, DE-FCO7-93ID12230 and DE-FC07-95ID113358 made significant advances in understanding the Lost Foam Casting (LFC) Process and clearly identified areas where additional developments were needed to improve the process and make it more functional in industrial environments. The current project focused on eight tasks listed as follows:

Task 1. Computational Model for the Process and Data Base to Support the Model
Task 2. Casting Dimensional Accuracy
Task 3. Pattern Production
Task 4. Improved Pattern Materials
Task 5. Coating Control
Task 6. In-Plant Case Studies
Task 7. Energy and the Environmental Data
Task 8. Technology Transfer

This report summarizes the work done on all tasks in the period of October 1, 1999 through September 30, 2004. The results obtained in each task and subtask are summarized in this Executive Summary and details are provided in subsequent sections of the report.

Task 1. Computational Model and Data Base. This task developed (1) a data base on foam degradation and (2) a physical model of the foam replacement process.

There were three subtasks that involved (1) conducting foam pyrolysis experiments, (2) examining pattern replacement using a real time X-Ray system, 3) observe defect formation in castings using the x-ray system, and (4) pattern replacement modeling. This task resulted in much more accurate computer simulations useful in minimizing defect incidence.

Foam pyrolysis experiments – These experiments measured parameters associated with foam replacement by molten metal and provided data needed to predict defect formation with mathematical models. The properties measured included pyrolysis gas evolution rates, effluent gas temperatures, gas pressures, and gas molecular weights. Degradation parameters associated with patterns having various degrees of surface quality were measured, and data on the degradation of pattern adhesives were gathered. The effect of pyrolysis heater geometry on pattern degradation was examined to be sure that the data being developed was accurate. It was determined that the heater geometry did not have a significant effect on foam degradation.

The database has been used in two computer codes to reduce scrap and casting defects. General Motors Corporation has developed a proprietary code to substantially reduce scrap and processing costs. These data have also been provided to Flow 3D, MagmaSoft, and Procast, and two of these codes have incorporated some of the data.

Real time X-Ray – An x-ray system was used to study pattern replacement by molten metal. Aluminum and iron casting studies were conducted. Effects of pattern fusion, pattern density, coating permeability, and glue joints were determined.

The x-ray system has provided valuable data on foam replacement. Pattern quality and consistency was found to be essential for controlling defect formation in castings. Perhaps 60% of the scrap produced in commercial foundries is associated with inconsistencies in patterns.

The x-ray system has also provided data on how folds and porosity occur in castings, and the information has been used by participants to improve castings quality. X-Ray data provides a benchmark for validating computer models of flow, fill, and pattern replacement. Quantitative data such as metal filling time, velocity and number of converging metal fronts have been extracted from video files and related to the pattern quality and the data used to improve computer codes.

Defect formation – Defect formation, especially fold and porosity formation, and effects of sprue design, process parameters, foam materials, alloy composition, metal superheat, hydrogen content, and visual interpretation of defective surfaces were investigated. Results of these evaluations are summarized as follows:

- Four sprue designs were evaluated without finding any significant difference in metal velocity or temperature. However, castings poured with foam sprues had more fold defects than those poured with ceramic sprues.
- Foam density, degree of foam bead fusion, and coating permeability effects on casting defect formation were evaluated in a statistical matrix involving 24 castings. Patterns having a low degree of fusion always filled at a high rate regardless of the coating type. Patterns coated with low permeability wash materials had fewer fold defects.
- Foam bead materials with and without bromine additives were evaluated. The additives substantially reduced the incidence of casting defects.
- The effects of aluminum composition on defect formation were investigated. The silicon concentration had no significant effect on the incidence of fold defects. However, castings produced with aluminum alloy 206, had significantly more casting defects than those produced with 319 or 356 alloys.
- The effect of metal superheat and hydrogen content on porosity was examined. As the superheat increased the metal velocity increased slightly, and fewer casting defects were produced.

- Data on root causes of defects in Lost Foam Casting were compiled. The database correlates the appearance of casting defects such as folds, blisters and internal porosity to the Auger analysis. The defects were found to contain various amounts of carbon, oxygen, aluminum and silicon that affect the appearance. Now, the appearance can be related to the defect cause.

Computational model – Flow Science and ESI ProCast are the two leading commercially available programs for simulating the Lost Foam casting process. In order to improve the commercial codes, experiments were conducted to develop a physical model of events occurring in the mold and algorithms that describe these events. Both ESI Procast and Flow 3D have incorporated some of the information and made significant progress in describing pattern pyrolysis.

ESI Procast released a new version of their code for simulating the lost foam process and provided UAB a copy for beta testing with sponsor companies. The new version allows inputs for coating parameters including coating thickness and permeability; pattern parameters including gas fraction, and glue joint effects; and heat transfer at the metal-foam interface to be varied and the effects calculated.

Flow 3D implemented a new pattern density model to simulate density gradients in patterns. The real time X-Ray system validated this code.

Task 2. Casting Dimensional Accuracy. Two sponsors having dimensional issues were examined to resolve dimensional variations. Previous work has shown that dimensional variation can be caused by excessive compaction table accelerations during the fill and compaction cycle and by sand thermal expansion. Distortion in one of the foundries was found to be caused by uneven sand filling in and around the pattern.

Three approaches are available to reduce distortion caused by uneven sand filling including:

- Adjust the fill and compaction cycle to ensure internal cavities in the pattern are filled at the same rate as the exterior to balance the compaction pressures on the pattern.
- Re-orient the pattern to allow easier pattern cavity filling.
- Mask the fill screen to achieve a more uniform fill of the flask.

Task 3. Pattern Production. This task focused on determining the effects of foam bead and pattern tooling on pattern permeability.

- A pattern permeability apparatus was developed as a tool for monitoring and controlling pattern permeability. The threshold pattern permeability affecting the metal flow was found to be about 1.0 cc/sec-cm^2.
- Validation experiments were conducted, and Arena-Flow-EPS was found to accurately describe the flow of beads into pattern cavities. The model has been found useful for tooling design and pattern defect analysis. A density model was implemented in the code in this phase

of work to make the modeling more robust.

- Pressure transducers and thermocouples were placed in a tool to measure the effects of molding parameters on pattern quality. It was found that the time the pattern is above 100°C affects porosity and the pattern density gradient, which in turn influences defect formation in castings.
- Patterns molded under different conditions were poured to determine effects of pattern variations on defect formation. The amount of open porosity in the pattern was directly correlated with casting scrap. This result was consistent with observations made with the x-ray equipment.
- A manual was developed that outlines the parameters that must be controlled during pattern molding and how these parameters can be controlled to make consistent patterns. The manual is available at AFS and UAB.

Task 4. Improved Pattern Materials and Processes. Modifying currently available pattern bead materials was explored to make the process more robust. Using a pattern pre-coat provided some guidance for recent research. Test castings poured using this pattern pre-coat exhibited an average of a 82% reduction in the number of surface folds and a reduction in average fold length by 42%.

A new bead material, referred to as "no fold", was introduced by a participating company. The new bead stock reduced the fold defect formation. Other foam stock including Polyurethane and PMMA were evaluated. None of the materials evaluated produced acceptable castings.

Several approaches were used in an effort to improve the pattern degradation and minimize casting defects. Coating and pattern additives were explored, respectively, and it was found that certain additives significantly reduced the incidence of casting defects. Pouring under certain atmospheres was also found to be beneficial. The patentability of these concepts is now being determined.

Task 5. Coating Control. Developments on coating consistency were continued in participating company plants. A high scrap rate on an engine block was associated with inconsistent permeability. Measurement consistency was examined and values obtained at UAB were compared to values obtained in a sponsor company. Correlations were made on two pieces of equipment using ten coating materials commonly used for producing iron and aluminum castings. Some effort was also directed at measuring system permeability, which includes both coating permeability and pattern permeability.

Pouring under the influence of vacuum was explored. The application of a vacuum might help remove pyrolysis products, but the high fill rates often increases the incidence of pyrolysis defects and metal penetration. No effective way was found to control the carbon pick-up in steel castings so work on this subtask was directed, with the agreement of consortium sponsors, to in-plant trouble shooting and technology exchange.

Task 6. In-Plant Troubleshooting and Technology Exchange. Two levels of training courses were developed and given at participating foundry companies. “Entry Level” was designed for new employees, and the “Process Level” course was designed for engineers and production personnel. Both courses provided insight and understanding of process control needed to minimize scrap.

Seven case studies conducted at participating foundries illustrate how to control the process and produce quality castings. These case studies not only helped improve the production yield, but also provided UAB with insight into real issues of interest to operating companies.

Task 7. Energy and Environment Data. Energy consumption and emissions data on the Lost Foam process were compiled from consortium members. In general, the environmental burdens associated with the Lost Foam and semi-permanent mold processes are similar. Overall, Lost Foam was found to be the most environmentally friendly process among semi-permanent mold and precision sand process.

Task 8. Technology Transfer. Technology transfer between UAB personnel and sponsors occurred in the form of meetings at four month intervals. Thirteen (13) sponsor meetings were held at UAB, at American Foundry Society (AFS) Headquarters in Chicago and in plants of sponsor companies. Additional meetings were held to review the research and examine its applicability in sponsor foundries. Technology transfer was also performed though conferences such as AFS Casting Congress, Lost Foam International Conference and TMS Annual Meeting.

ADVANCED LOST FOAM CASTING TECHNOLOGY
2000 - 2004 Final Report

OBJECTIVE

The purpose of this project was to advance the state of the art for the Lost Foam (LF) Casting process and improve the competitiveness of the U.S. metal casting industry. Activities to accomplish these objectives are conducted through a Lost Foam Technology Center located at the University of Alabama at Birmingham (UAB). The Center is focused on developing and demonstrating advanced casting technology and transferring this technology to project participants. Participants include casting designers, foundry suppliers, equipment producers, producing foundries and casting users. This project provides a means for designers, manufacturers, and purchasers/users of castings to advance the science of casting production. The project gives participants contact with leaders in the industry and helps develop the best available technology.

ACCOMPLISHMENTS

1. Computational Model and Data Base

The objective of this task was to develop a data base of liquid/gas ratio, energy of degradation, and power density for patterns used in producing both aluminum and iron castings. The technology developed allows new materials to be evaluated in a straightforward manner and with a minimum of foundry casting experiments. The resulting data is used in a computational model to describe pattern replacement. The second objective was to understand and minimize defects associated with pattern replacement (pyrolysis). The computational model predictions were compared to experimental casting data to validate the model.

1.1 - Pattern Material Degradation Properties Data Base

Foam pyrolysis studies focused on mass and heat transfer in the kinetic zone between molten metal and the pattern during pouring and developed data for a mathematical model. This subtask was accomplished through three tasks conducted at UAB (University of Alabama at Birmingham) and UMR (University of Missouri - Rolla):

1. Pattern degradation during Foam Pyrolysis
2. Pattern replacement visualization using real time x-ray technology
3. Relating pattern degradation to casting defect formation

Achievements in these tasks are summarized as follows:

1.1.1 Characterization of Pattern Degradation during Foam Pyrolysis

1.1.1.1 Heater Material

An effort was made to extend the temperature capability of the foam pyrolysis apparatus to iron and steel pouring temperatures (1600°C) using silicon carbide (SiC) heaters. SiC offers resistance to oxidation and is a relatively low cost material. A 0.95 cm diameter SiC heating element was instrumented with platinum/rhodium thermocouples attached to the front and back heater faces. Pyrolysis experiments were conducted at 1600°C on EPS, PMMA, and a copolymer containing 30% PMMA/70% EPS covering the density range from 19.4 to 21.6 kg/m^3 (1.21 to 1.35 pcf)- at a velocity of 5.1 cm/s.

A thermal gradient of approximately 800°C developed in the heater as PMMA was pyrolized. The gradient could be reduced by either using a higher thermal conductivity heater or reducing the heater thickness by a factor of 10. Reducing the heater thickness was not feasible because of machining problems with SiC.

Carbon was found to be deposited on the heater front face. Carbon buildup ranged in thickness from less than 1 mm for copolymer patterns to 3 mm for EPS patterns. The carbon layer insulated the heater, and caused overheating and burnout of the front thermocouple. The conclusions reached were that SiC is not a feasible heater material because of its low conductivity and carbon deposition caused the heater to fail.

1.1.1.2 Heater Size and Shape

Experiments were also conducted to evaluate the effect of the heater size and shape on foam pyrolysis. Heater assembly of the foam pyrolysis apparatus is shown in Fig. 1. The residence time of the polymer in the kinetic zone should depend on the size and shape of the heater. Two sets of experiments were conducted using both concave and convex heaters. The experiments were videotaped to study mass and heat transfer in the kinetic zone.

The heater shape was not found to have an effect on power density or specific degradation energy. Gas fraction for the concave heater was about 15% higher than for the convex shape. Based on the visual observations and analysis of the data, the higher gas fraction produced by the concave heater was probably a result of liquid degradation as pyrolysis products built up on the heater face outside the kinetic zone.

Heater shape did affect the escape of liquid pyrolysis products from the kinetic zone. The convex shape facilitated flow around the heater in comparison to the concave heater. The heater width did not have a significant effect on the gas fraction.

It was concluded that the effect of heater geometry on the residence time of the polymer in the kinetic zone was too small to observe. This implies that the channel thickness and metal front shape is not critical in a computational model for pattern replacement by molten aluminum.

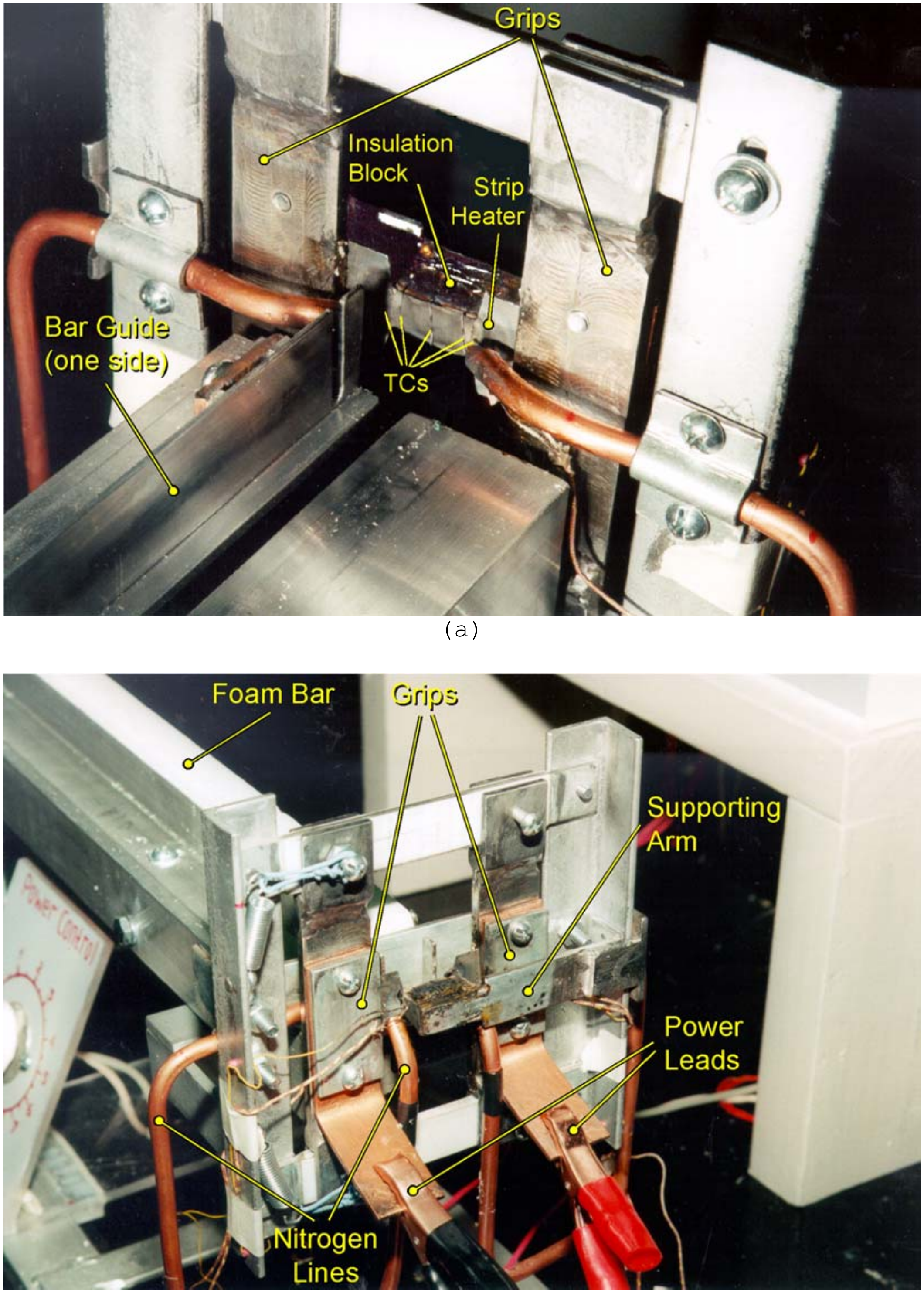
Grips
Insulation Block
Strip Heater
Bar Guide (one side)
TCs
Foam Bar
Grips
Supporting Arm
Power Leads
Nitrogen Lines
Power Control

(a)

(b)

Figure 1. Heater assembly of foam pyrolysis apparatus. (a) Front view, (b) rear view. TCs = thermocouples.

1.1.1.3 Gas Generation Regimes

New data was obtained using the 1 cm wide heater in the temperature range of 550-800°C. The degradation data in this range is important for modeling Lost Foam because this is the range of temperatures used to make aluminum castings. Three gas generation regimes were found:

(a) Pattern melting, characterized by small gas fraction ($F_{gas} < 10\%$) and occurring at heater temperatures below 590-620°C;
(b) Gas film formation, at $T_{heater} > 680\text{-}710°C$ with $F_{gas} > 30\%$;
(c) Transition from melting to gas film formation with gas fractions varying from 10% to 30%.

The transition points between the gas generation modes appeared as discontinuities in the gas fraction curves.

1.1.1.4 Gas Generation Rates

A gas generation (vaporization) rate (R_v, measured in grams of gas produced per second from a cm^2 of degrading pattern surface), was introduced to describe the volume of gas produced in the kinetic zone during pyrolysis. Recession velocity had no effects on gas generation rate at temperatures below 650°C. At 650°C, there was an inflection, followed by a rate, dependent on the recession velocity. Higher R_v values and steeper slopes were associated with higher recession velocities.

The gas generation rate at recession velocities of 1.78 cm/s and 3.33 cm/s leveled off at temperatures between 1050°C and 1150°C. This was a result of a thick gas film between the heater and the pattern which reduced the heat transfer rate.

The gas generation rate data were analyzed using an Arhenius expression, and it was found that the gas generation rate at temperatures in the range of 550-670°C followed a straight line for different velocities. The pyrolysis activation energy was found to be 131 kJ/mole. This value was about 30% below the value found in the value of 192.6 kJ/mole reported in the literature for polystyrene. The discrepancy was attributed to the difference in temperature between the polymer and the heater surface caused by the insulating gas film.

The gas generation rate data deviated from the straight line above about 640°C at V_{rec}=1.78 cm/s and above 670°C at V_{rec}=3.33 cm/s. The deviation points correspond to the discontinuities in the gas fraction curves and indicate a change in the gas generation regime–i.e., the development of an insulating gas film between the heater and the pattern.

1.1.1.5 Temperature of Gaseous and Liquid Pyrolysis Products

Experiments were conducted to measure the temperature of the pyrolysis products in the kinetic zone and estimate the gap between the metal and the pattern. The temperature of the gas escaping the kinetic zone at foam recession rates of 1.78-3.33 cm/s increased from 450°C to 730°C as the heater temperature was raised from 620 to 1050°C. The temperature of the liquid fraction was approximately 315°C at a heater temperature of 600°C and 446°C at a heater temperature of 1000°C.

The gas temperature measurements did not indicate any effect of the recession velocity on gas temperature. The average gas temperature was found to be approximately 380°C and 700°C at a heater temperature of 600°C and 1050°C, respectively. The standard error of the data about the fit was 58°C.

1.1.1.6 Resistance Pressure of Pattern Degradation

A load cell was used to measure the force between the foam bar and the pyrolysis heater. The force data was used to calculate the pattern degradation resistance pressure and put in a computer model to predict metal filling velocity.

Pyrolysis experiments were conducted to develop pattern degradation resistance data for EPS. Patterns were pyrolized using heater temperatures between 550-870°C using recession rates of 1.93 cm/s and 3.52 cm/s. The pressure data exhibited a hyperbolic response at pressures near 150 g/cm^2 (2.13 psi) at 555°C, 27 g/cm^2(0.38 psi)at 720°C, and 6 g/cm^2 (0.09 psi) at 850°C. The pressure values at higher recession rate of 3.52 cm/s at heater temperatures of 650-800°C were 6-7 times higher than those at the lower recession rate. The data were in good agreement with data obtained on pattern recession rates observed in 319 aluminum castings.

1.1.1.7 Molecular Weight of Foam Pyrolysis Products

Samples of EPS liquid residue were collected and the molecular weight (Mw) of the residue samples determined. It was found that residue molecular weight was about 25% of the Mw of virgin EPS (75,000 vs. about 300,000). The molecular weight was independent of the heater temperature and pattern recession rate.

1.1.1.8 Effects of Molded and Cut Pattern Surfaces

Several experiments were conducted to determine the heater/foam interface using patterns with molded and cut surfaces. EPS patterns were saw cut and tested at recession velocities of 1.78 cm/s and 3.33 cm/s in the temperature range of 600-1000°C. The results were compared with data from seven molded EPS patterns having an average density of 25 kg/m^3. Patterns recession rates were 1 cm/s, 1.8 cm/s, and 3.4 cm/s, using heater temperatures of 600°C and 780°C at each velocity.

The heater/pattern interface on the molded bars was smoother than the interface produced in saw cut patterns. Fewer gas bubbles broke through the molded surfaces compared to cut surfaces. A molded pattern surface provides less effective area for gas escape compared to a saw cut pattern.

1.1.1.9 Effects of Foam Pattern Fusion

Experiments were conducted to determine if gases produced during pattern pyrolysis could escape the kinetic zone through a pattern. EPS patterns were pyrolized and the events video taped to observe gas flow through the pattern. The heater temperature varied from 660°C to 735°C.

Patterns having a low degree of fusion degraded with an average recession velocity of 2.8 cm/s, about 25% faster than the normally fusion patterns. Analysis of the pyrolysis videos showed that holes appeared in the pattern near the heater. The holes appeared to be caused by hot gaseous degradation products escaping through the pattern ahead of the kinetic zone. Fewer holes were observed during pyrolysis of normally fused patterns. This data indicates that pattern permeability is an important factor affection gas escape from the metal-pattern interface, and it must be controlled to achieve consistent casting quality.

1.1.1.10 Degradation of Pattern Adhesives

Degradation data is needed on pattern adhesives to serve as the baseline for the development of new materials. Two types of experiments were conducted where glue joints were placed transverse to the test pattern length. The joint thickness ranged from 0.17 to 0.42 mm and heater temperatures of 600 and 700°C were used. The results are summarized as follows:

- The movement of a glue joint into the hot zone caused a significant decrease in the rate of pyrolysis. Glue joints with a thickness of 0.16-0.28 mm, produced contact times of 0.2-0.33 s.
- Higher driving pressures and heater temperatures reduced the contact time.
- Glue joints imposed an additional thermal load and reduced the heater temperature by 30-50°C. The same event occurs in molds as metal contacts glue joints.

The degradation properties of some protein and new hot melt adhesives were also evaluated. The protein (gelatin) adhesives may be superior to hot melt adhesives due to their lower working temperature (43-54°C) and longer tack time.

A glue joint was put in EPS patterns transverse to the bar length. The pyrolysis of two hot melt and two protein adhesives, designated as HM-30-7176, HM-30-7177, P-500R-125, and P-600R-137, were examined. The glue joints evaluated ranged in thickness from 0.16 to 0.43 mm.

The bars containing the glue joints were pyrolized under conditions representing those encountered when pouring aluminum. The degradation parameters measured were the contact time of heater with glue joints and heater temperature change during contact.

The results are summarized as follows:

- Degradation of all hot melt glue joints occurred by melting and vaporization and reduced the heater temperature about 33°C during contact, which lasted about 0.29 s.

- No significant differences in degradation parameters were found between different hot melt adhesives. Higher temperature drop was produced by thicker joints as expected.

- Protein adhesives degraded by char formation. The char created some thermal insulation and increased the contact time with the heater.

- Protein adhesives do not appear suitable for use at the present time. Water solubility of modified proteins is another obstacle for the use of these adhesives.

1.1.2 Examination of Pattern Replacement using Real Time X-Ray Technology

1.1.2.1 Real Time X-Ray Apparatus

The real-time x-ray system, used to examine events inside molds during filling, is comprised of two X-Ray units. Overview of the X-Ray unit and set up for metal pouring are shown in Fig. 2. The first unit consists of a 320 kV tube having a source spot size of 0.8mm × 0.8mm and a 9″ tri field image intensifier with a Sony XC75CCD camera. The operation of this unit is integrated by a microprocessor console.

The second unit consists of a 160 kV micro-focus X-Ray tube with a focal spot size of 5 to 200 microns and an A-SI (amorphous silicon) digital detector. The detector has an active area of 203 × 254mm and has a pixel array that is 1997 × 2592 in the x and y axes and contains a total of 3.1 million pixels. Each pixel can provide 12 bit images or 4066 shades of gray with a frame capture rate of 7/second. The X-Ray systems are located in a room of steel-lead-steel construction. The x-ray control and data acquisition systems are located in an adjacent room.

As the molten metal replaces foam patterns, X-Rays pass through the flask and project onto a cesium-iodide (CsI) fluoroscopic screen which produces visible images. The images are recorded using a 30 frame per second camera connected to a VCR. Video images can then be transferred to a computer controlled image processor for image processing, such as image enhancement and color-coding.

The molding material used is usually silica sand with a grain fineness number (GFN) of 55. Sand is rained into a flask around a pattern while the flask is vibrated vertically or horizontally to achieve uniform compaction. A pouring apparatus with remote control pours the liquid metal inside the x-ray vault. The crucible is rotated by a motor-sprocket-chain at rates of from 0.2 rpm to 10 rpm depending on the desired pouring rate.

Many of the castings poured were 6inch × 8inch × 0.3inch (152mm × 203mm × 8mm) plates. The alloy poured was usually 356 Aluminum poured at 1450F. Triplicate castings were usually poured to ensure data repeatability.

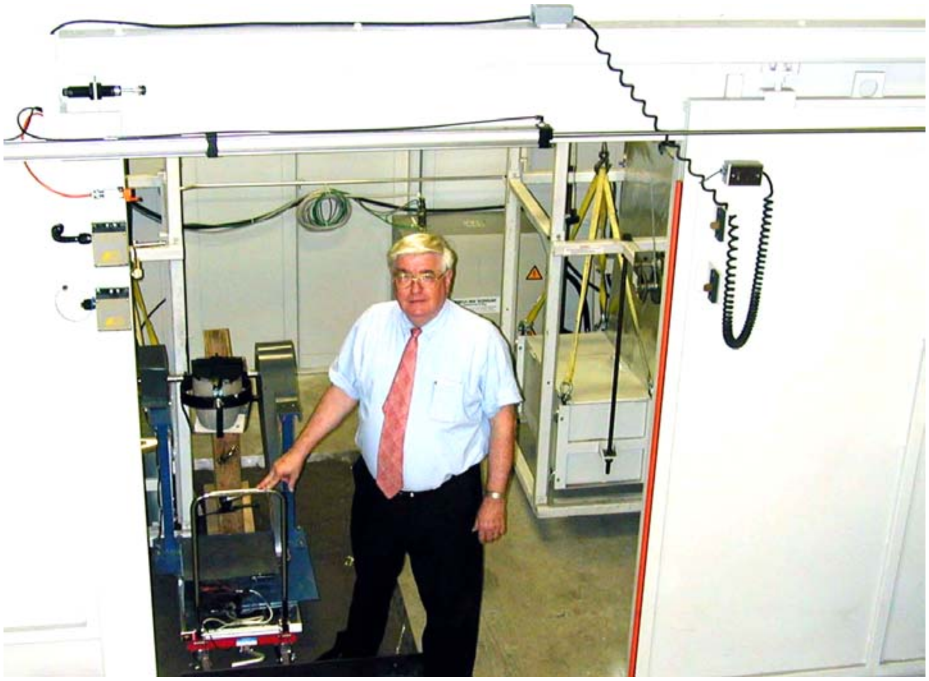

(a)

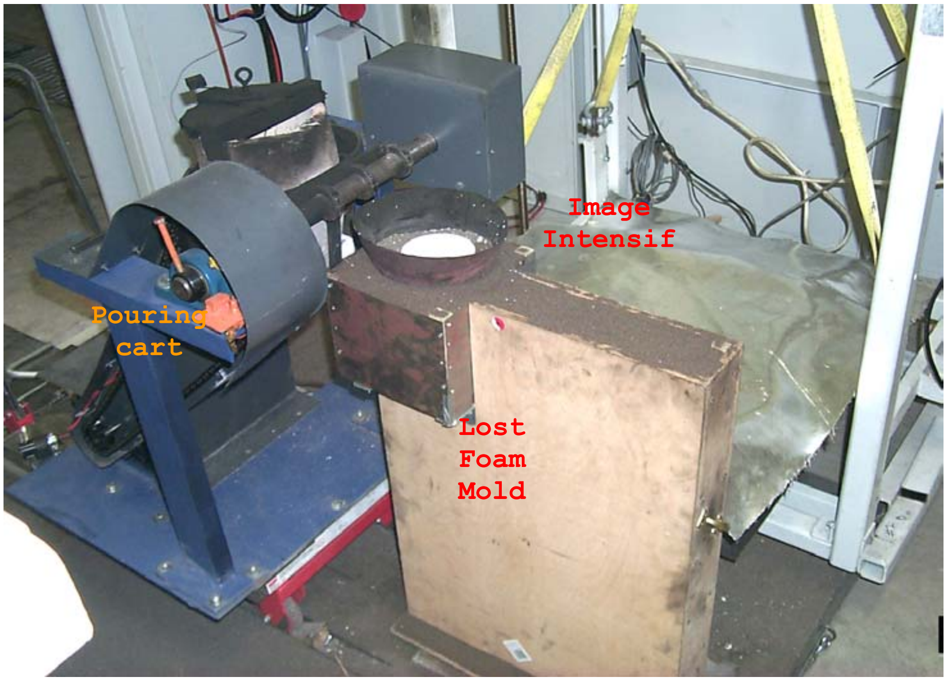
Image
Intensif
Pouring
cart
Lost
Foam
Mold

(b)

Fig. 2. Set-up for real time X-Ray observation of metal filling of lost foam castings. (a) Overview of the real-time X-Ray facilities; (b) set up for the pouring.

1.1.2.2 Metal Filling of Lost Foam Aluminum Castings

Experimental Matrix

Experiments were conducted to determine the effects of EPS pattern density and degree of fusion (open porosity), coating permeability, and pattern glue joints on pattern replacement and casting defect formation. Most experiments were conducted on 8 mm thick plates. Pattern density maps were obtained using a capacitive probe, an Industrial Analytics (IA) x-ray technique, and Lixi, also an x-ray technique. Sequential maps of metal front profiles made from x-rays were compared to pyrolysis traces on the surface of the resulting castings.

Data Acquisition

Pattern property parameter - Pattern fusion: Two degrees of pattern fusion were considered. One was referred to as "low fusion", where beads were in contact but not expanded sufficiently to eliminate voids between beads, and the second was referred to as "normal fusion" where beads were sufficiently fused to produce a smooth pattern surface.

Pattern property parameter - Foam density map: The patterns were scanned at quarter inch intervals with a small diameter X-Ray beam and the density of the pattern measured from the transmitted x-ray intensity. From these maps, local densities and density gradients in patterns could be defined.

Coating parameters - Dry coating weight on patterns and coating permeability values were determined. Coating permeability was measured using procedures developed by Littleton and published in 1997.

Metal front profiles - Metal front profile maps were made by printing x-ray images made during filling at 6 frame intervals (0.2 second). These maps allowed the metal front profiles to be examined without replaying the video repeatedly. Changes in the metal front profile were clearly seen in the maps made at 0.2 second intervals. Also, the instantaneous metal fill velocities could be obtained from the maps. These velocities provide accurate data for validating computer models.

Two characteristic parameters were developed from the maps of metal front profiles: 1) Number of converging metal lines. 2) Average metal filling velocity along the plate centerline. The average velocity along the centerline of the plate was used to compare the effects of experimental parameters on casting quality.

Pyrolysis traces and defects - The liquid pyrolysis products produced during foam pattern replacement produce lines on casting surfaces. The distribution of the lines and defects (folds and blisters) were recorded using a digital camera and located on a coordinate grid. The number of casting defects was taken as the characteristic parameter.

Coating Permeability and Pattern Fusion

The data indicates that coating permeability and degree of pattern fusion(open porosity) have significant effects on the metal front shape, and metal velocity into the mold, and defect formation. Metal replacement of low fusion patterns was faster and more unstable than replacement of normally fused patterns. Patterns having a low degree of fusion consistently produced jagged metal fronts and fold defects, while normal fusion patterns produced smooth (stable) metal fronts and much less fold defects. Patterns having the same degree of fusion that were coated with materials having a high permeability resulted in high metal velocities and large amounts of liquid degradation products that produced defects in castings. Some liquid pyrolysis products floated in the casting cavity and others produced surface defects.

Foam Density

The nominal pattern density was not found to have any statistical effect on the velocity for replacing patterns having a low degree of fusion. High density areas in patterns of a low degree of fusion significantly reduced metal velocities, produced merging metal fronts, and increased casting defects. Effect of foam density gradient on metal filling and metal filling on fold defect formation are shown in Fig. 3. However, high density areas in normally fused patterns did not markedly affect metal velocity.

Coating Permeability

Coating permeability also had a significant effect on metal velocity and the occurrence of defects. The coating must have proper permeability in order to minimize converging metal fronts and the formation of bubbles of liquid pattern pyrolysis products. A pre-coat sealer on the surface of a normally fused pattern decreased the filling velocity by about 30%.

Glue Joint Effects

Section and perimeter glue joints were found to decrease the metal velocity and increase the number of converging metal fronts. Perimeter glue joints did not have any significant effect on the metal filling velocity or the number of converging metal fronts.

Metal Filling and Casting Quality

Comparisons of metal front profiles with pyrolysis traces and casting defects showed that converging metal fronts lines were related to pyrolysis traces and fold defects. These results were consistent with the previous studies that correlated fold defect occurrence to the pattern replacement velocity.

Cracked Coatings

Effects of cracked coatings were determined by deliberately scratching coated patterns. The scratches changed the metal front profile from smooth to irregular and resulted in more casting defects. Cracks and similar coating defects must be minimized.

Metal Front Profile

Metal front profiles were recorded using slices removed from low and normally fused patterns. Metal front profiles obtained from normally fused patterns were flat and produced the fewest casting defects. Metal front profiles obtained using patterns with low degree of fusion were concave and produced converging metal fronts, which tended to produce more defects.

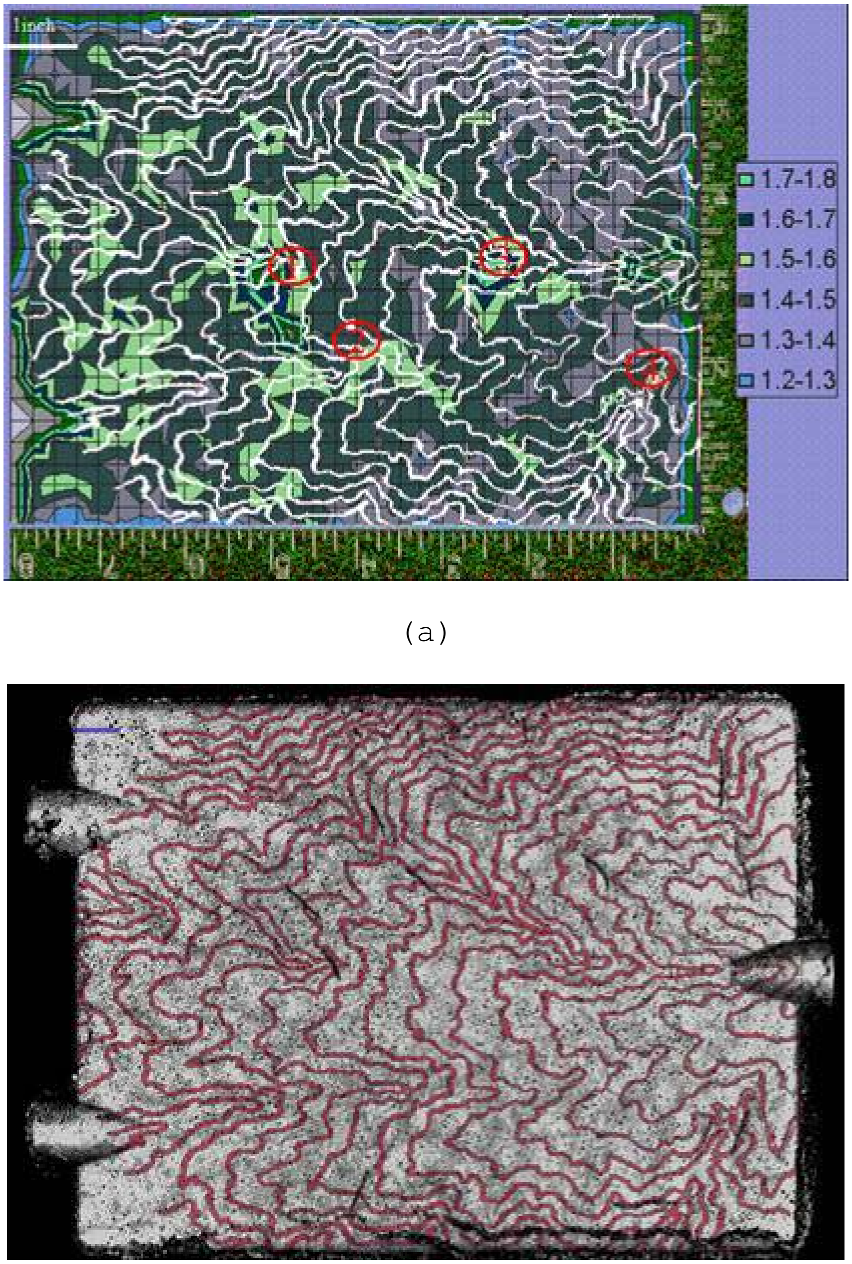

(a)

(b)

Fig.3. Quality of casting poured with low fusion pattern with 1.3 lb/ft3 density. (a) overlay of map of metal front profile on pattern density map; (b) overlay of map of metal front profile on casting surface.

Pattern replacement with no pattern coating

Pattern replacement under these conditions resulted in high metal velocities, irregular metal fronts, bubble formation, and gas holes. This is the same type of fill pattern as when filling of patterns with high permeability coatings.

Metal filling through hollow sprues

The average replacement velocities seen with patterns poured with hollow sprues was higher than similar patterns poured with foam sprues.

1.1.2.3 Interior Quality of Lost Foam Aluminum Castings

The interior quality of the 6 inch x 8 inch UAB aluminum plate castings was inspected using digital x-rays. Porosity bands were found in most castings poured with normally fused patterns, except for some special conditions. Patterns having a lower degree of fusion produced smaller bands of defects. A reduced casting thickness was associated with pyrolysis products entrapment between the coating and metal at converging metal fronts.

Experiments were conducted where variations were made in plate thickness, pouring temperature, and gating arrangement to determine causes of the line of porosity in cast aluminum. Porosity bands were found in plates with thicknesses of 4, 8, and 12mm, but the porosity was worse in the thicker castings.

The effect of pattern pre-coating and glue joints on the occurrence of porosity lines was examined. The porosity bands were reduced in severity but still present in castings produced using low fusion patterns with a pre-coat. The pre-coat reduced the metal velocity, generating less liquid pyrolysis products. Glue joints in normally fused patterns also slowed the metal fill rates and reduced the porosity band. Decreasing the amount of glue similarly decreased the porosity.

Studies of the effect of coating permeability, thickness, and surface condition on defect formation indicated that the metal front profile changed from smooth to fingered as the coating permeability increased. Smooth filling eliminated the porosity band.

The porosity defects were examined using a stereo microscope and SEM, and most of the pores were found to be caused by gas. Some shrinkage and hydrogen related pores were present, but most were caused by gas from pattern pyrolysis.

The effect of top gating on porosity bands was determined using 8 and 24mm thick patterns having a density of 1.3pcf. Top gating produced bands on one or both sides of test castings.

The porosity band appears to be the result of entrapped gas from pattern pyrolysis products in the molten metal. The bubbles float toward the top casting surface and agglomerate just below the solidified metal along the top edge of the castings.

1.1.2.4 Effects of Pattern Tooling on Metal Filling

A series of patterns having dimensions of 10×200×180mm were produced in two types of tools and the effect on defect formation was determined. Both low and normally fused patterns were blown in both vented and ventless tools. The permeability of each pattern was measured; each pattern was coated, and then poured with aluminum alloy. Pattern replacement was viewed using the x-ray system. Metal front profile maps were made and overlaid on the permeability maps to determine the effects of the tooling on pattern replacement and defect formation. Three patterns were examined under each set of experimental conditions to ensure data repeatability.

Vented tools produced slow and smooth metal fronts when the patterns were well fused, and fingered metal fronts when the patterns were not well fused. Ventless tooling produced fingered metal fronts with both low and high fused patterns.

Pattern permeability maps were then overlaid on metal front profile maps. The permeability of patterns molded in vented and ventless tools was found to be quite different. When metal replaced the pattern, the metal followed the regions of higher permeability and produced erratic metal filling behavior. The patterns produced in ventless tools generally had higher density variations and more irregular filling.

Foam pyrolysis traces on casting surfaces were recorded as a measure of surface quality. Pyrolysis traces on the back side of patterns were more than on the fill gun side of the pattern. This was probably caused by a non symmetrical permeability on the two sides of the patterns. The back sides of patterns had higher permeability values compared to the fill gun side. Castings poured with well fused patterns made in ventless tools are cleaner than equivalently fused patterns molded in vented tools. This suggests that the highly fused vent area in patterns made in vented tools may be a site of liquid pyrolysis accumulation.

1.1.2.5 Metal Filling of Lost Foam Iron Castings

Several modifications were made to the x-ray vault, metal melting and pouring equipment, and pattern coating procedures to examine pattern replacement when pouring iron. The parameters examined included degree of pattern fusion, pattern density, coating permeability and glue joints. The UAB plate patterns were poured using bottom gating systems. Type K thermocouples and pressure transducers were used to measure the iron temperature and the amount of vacuum on the flask.

The degree of pattern fusion had a significant effect on metal filling. Normally fused patterns filled smoothly. Patterns having a low degree of fusion filled with "w" shaped metal fronts and lustrous carbon defects formed at the converging metal fronts. Patterns with a low degree of fusion produced higher fill velocities larger casting defects. The foam density had a mixed effect with higher density foams producing lower metal velocities and smaller defects. Pattern density had no significant effect on metal velocity or defect area at low degrees of fusion.

Two coatings having permeabilities of 42.7 $cm^3/(cm^2.s)$and 37.0 $cm^3/(cm^2.s)$ were used to examine the effects on filling of iron castings, but no statistical effect on metal velocity was found in this range. However, high permeability coatings reduced the incidence of lustrous carbon defects. Glue joints parallel to the metal filling direction distorted the metal front, and defects were reduced in low fusion patterns but increased in normally fused patterns having glue joints.

1.1.3 Pattern Degradation and Casting Defect Formation

1.1.3.1 Effects of Sprue Design

Twenty-four (24) flange castings were poured to determine effects of metal velocity and analyze the defects produced. The sprue types included an un-tapered hollow sprue, a tapered hollow sprue, a solid foam sprue, and a "hollow" foam sprue. Castings were poured in duplicate with a filter, with an aluminum plug, or with both a filter and a plug using each type of sprue.

The pyrolysis-related defects in the castings were analyzed and a data base on defects constructed which included the frequency of occurrence and location within the casting. The defect colors varied, and may be related to the composition and/or defect origin. As a consequence, the defect colors were mapped and correlated to the casting parameters. Selected defects were subjected to Auger and SEM analysis.

It was found that the metal velocities were slightly higher when hollow sprues were used compared to solid foam sprues. Straight hollow sprues produced the highest velocities. However, differences in metal velocity were small, and the sprue type had a very small effect on casting quality. Low permeability coatings were used so few blisters or pores were found in the castings. However, folds were found in all castings, and more folds were found in castings produced with foam sprues (either solid or hollow) than in the castings produced with ceramic hollow sprues. The largest number of folds was found in castings produced using hollow foam sprues.

The smallest number of folds was found using hollow tapered ceramic sprues, which produced fewer liquid pyrolysis products and less turbulence during sprue filling. The effect of various filter/plug combinations on fold formation was inconsistent. Folds tended to be concentrated in the last half of the casting filled with metal, while blisters normally formed in the first half of the casting to fill.

1.1.3.2 Effect of Process Parameters on Defect Formation

A matrix of 24 flange castings was poured using two foam densities (1.1 pcf and 1.6 pcf), high and low degrees of fusion, and high and low coating permeability. Castings were poured at 800°C using 319 aluminum.

Coating permeability ranged from 5 to 100, as determined by the GM Screen Test procedure. In general, the 1.6 pcf, patterns having a low degree of fusion filled at higher rates irrespective of the coating permeability. Un-diluted low permeability coatings produced the highest metal velocities.

Defect analyses showed that the low permeability coatings produced fewer defects. The castings had lower blister areas and fewer fold defects.

Auger analyses were made on selected defects, and high carbon concentrations were found in areas with gold/brown discolorations. Less carbon was present on silver-colored surfaces. The darkness of the surface may depend on the amount of carbon present, i.e. darker brown or gold surfaces have thicker carbon layers compared to the lighter colored areas. An Auger analysis made on a "brown smear" on a casting had a thick carbon layer. A sample of low permeability, un-diluted coating was examined using an SEM both before and after pouring a casting, but no significant difference in the structure could be found.

1.1.3.3 Effect of Foam Materials (T180 and T185)

T180 and T185 bead stock are identical EPS beads in molecular weight and size, but T185 "no fold" beads contain an additive to reduce the molecular weight of EPS pyrolysis products. A box pattern was used, and the effects of four factors including foam density (1.3 pcf and 1.6 pcf), degree of fusion (high and low), bead type (T180 and T185), and coating type (low perm/low liquid absorption and low perm/high liquid absorption) were examined.

The first task examined the effect of the sprue type. A 2×2 full factorial design was used to examine sprue and pattern density effects. The sprues were tapered ceramic, and the pattern densities were 1.1 and 1.86 pcf.

It was found that metal velocity did not significantly change with foam density when using the small tapered sprue; however, the pattern density did affect the metal velocity when the large tapered sprue was used, probably because the large sprue could be filled faster and kept full during pouring. Small tapered ceramic sprues were used in subsequent experiments.

Two box patterns were attached to a common sprue and poured with 356 aluminum at 760±20°C. Ninety-six (96) castings were produced and evaluated. It was found that the use of T185 beads reduced the metal velocity and the number and size of casting defects formed. The use of a low permeability/high liquid absorption coating also decreased the metal velocity. Both normally fused and high density patterns decreased the metal velocity.

The defect size was smaller when using normally fused patterns made from T185 beads and applying a low permeability/high liquid absorption coating. As the pattern density increased, the size of the defects decreased in castings made with low fusion patterns, but increased with density when using normal fusion patterns. Regardless of the type of coating used, patterns produced using the T185 beads produced castings with smaller defects.

Using a statistical analysis, the parameters having the greatest effect were the bead type (36.0%) and degree of fusion (35.3%). The use of T185 decreased the total defect area from 30 mm^2 to about 12 mm^2. The highly fused pattern also decreased the total casting defect area.

1.1.3.4 Effect of Alloy Composition

The current model describing pyrolysis defect formation suggests that the freezing range of the alloy contributes to the types of defects produced. This study was conducted using a Al-Si alloys containing 1%, 6%, 11%, and 12.3%Si. Pure aluminum and an Al-50%Si master alloy were used as charge materials. All castings were poured at approximately 125°C above the respective alloy liquidus temperatures. Two flange castings (see Fig. 4) of each composition were produced, velocities measured, and defects examined.

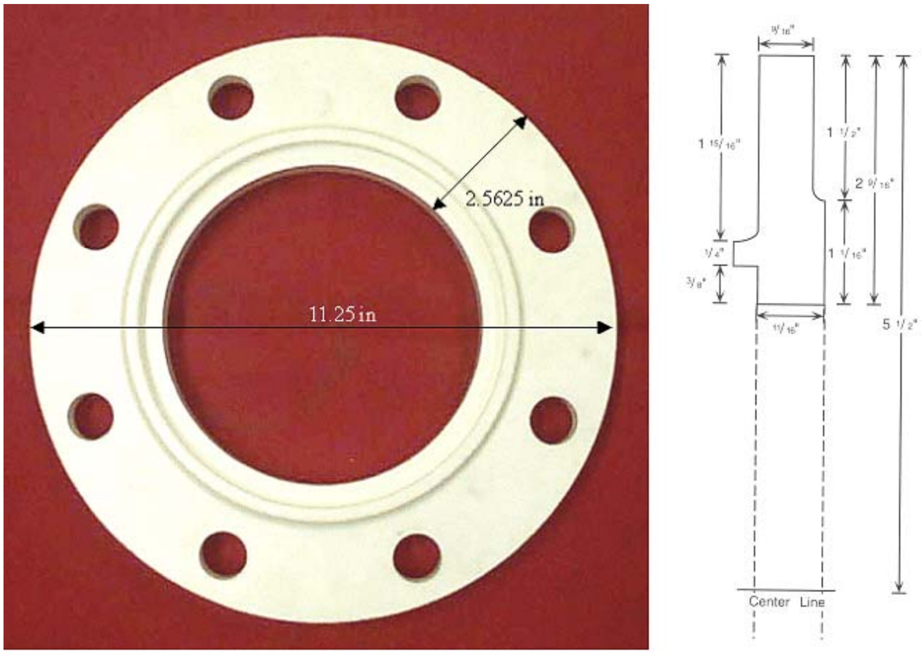

Figure 4 Top view of the flange pattern with a cross-sectional view on the right.

The 1% Si alloy having the longest freezing range produced the highest metal velocity. Higher silicon concentrations produced similar but lower fill velocities. The 6%Si alloy had a lower liquidus as well as a shorter freezing range. The 11%Si and 12.3%Si alloys were near-eutectic alloys with the lowest liquidus and shortest freezing range.

Folds, blisters, and pores were found in most castings. Folds and pores were concentrated opposite the ingate where the metal temperature was near the liquidus temperature, and blisters were concentrated near the gate. The silicon content did not have a significant effect on fold defect severity. However, blisters were severe in the 1%Si alloy and were near zero at the highest silicon concentration.

No internal pores were observed in the 1%Si and 6%Si alloys, but a large number of pores were present in the near-eutectic alloys. These results do suggest that the solidification sequence affects the nature of the pyrolysis defect.

A designed experiment was also conducted to determine if there were different kinds of defects produced by different casting alloys including 206, 319 and 356. Flange patterns (see Fig. 4) were used with densities of 1.3 and 1.6 pcf and prepared with T180 and T185 (no fold) beads.

The results again confirmed that castings produced using T185 patterns have significantly fewer casting defects. Castings poured using alloy 206 exhibited significantly more casting defects than those poured with 319 and 356 alloys. The high density T185 patterns produced a higher metal fill velocities compared to those produced with T180. This indicates that the additive in T185 beads reduces the molecular weight of the liquid pyrolysis products.

1.1.3.5 Effect of Superheat and Hydrogen Content

Experiments were conducted to study the effects of hydrogen content and superheat of the melt on defect formation in castings. Eighteen (18) flange patterns described above were cast at three superheat values and three different contents. The superheats were 75°C, 150°C, and 195°C. The hydrogen contents ranged between 2 and 20 percent.

A good correlation was found between superheat and defect formation but not with the hydrogen concentration. As the superheat increased, the metal velocities increased by about 0.25 cm/s, and this increased both the number of folds and internal pores. The best results were obtained with a superheat of 75°C and 150°C.

Higher superheat values also increased the number of blisters. This was probably a result of the fact that more superheat allowed more of the pyrolysis products to float to the surface and be entrapped just beneath the metal skin. The folds, blisters, and internal porosity occurred randomly in the casting. Hydrogen pores were also randomly distributed in the castings irrespective of the hydrogen concentration.

1.1.3.6 Defect Database

Samples of different defects were collected and analyzed by Auger (AES) and Scanning Electron (SEM) and the results are put in the defect data base. One of the databases is demonstrated in Fig. 5. Auger analysis indicated that black pores were coated with a thick layer of carbon and contained very little aluminum oxide. The carbon layer thickness may increase in larger pores. SEM analysis also suggested the presence of carbonized pyrolysis products having a smooth skin.

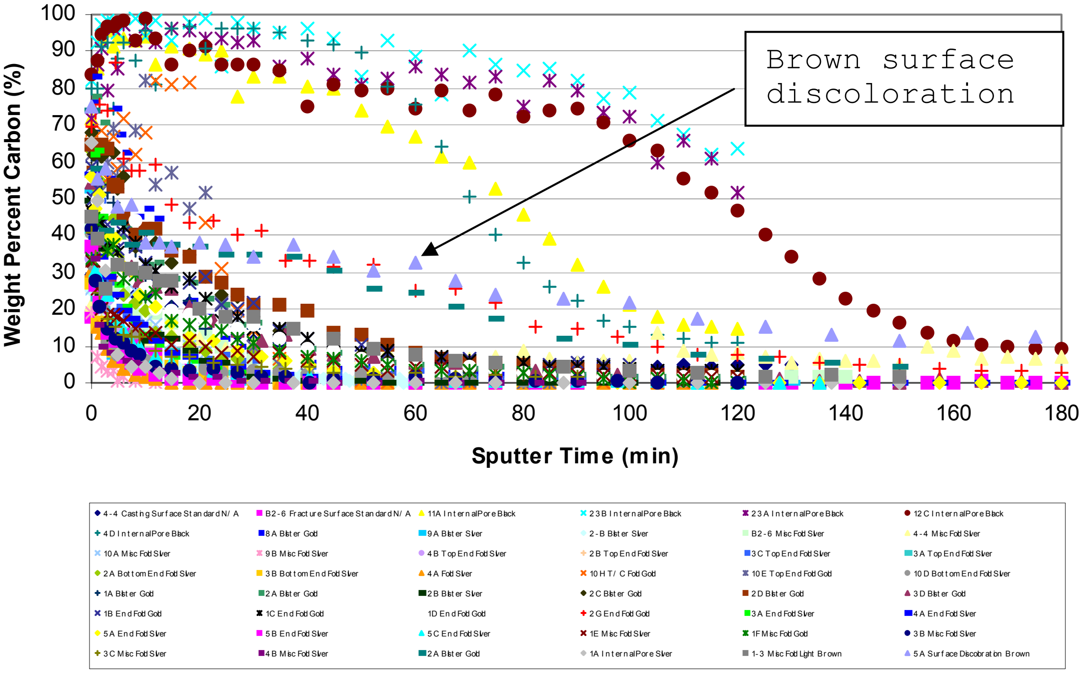

Fig. 5. Comprehensive AES depth profile showing weight percent carbon versus sputter time.

Folds exhibited wrinkled surfaces appearance under both optical and SEM microscopes. Some of the folds had a gold color, and Auger analysis found that the fold contained a thick layer of carbon. In "silver" colored folds, the carbon layer was thinner, and the carbon content appeared to be lower. The carbon layer suggested that these folds may be composed primarily of aluminum oxide, with only adventitious carbon present. An oxide layer was found beneath the carbon layer on both types of folds.

1.2 Computational Model

The objective of this work was to develop a fill and solidification code that accurately described the defect forming events of metal/pattern exchange as described in 1.1. The initial plan was to develop the algorithms based on parameters controlling the metal/pattern replacement and then put these algorithms into a commercial code. A decision was made, however, to simplify the modeling by using experimental data to describe the metal/pattern replacement using data from the Pattern Pyrolysis Apparatus. The use of the experimental data significantly shortens the computation time. The x-ray system described in 1.1.2.1 was used to verify the code predictions.

1.2.1 Existing Codes

Flow-3D and ProCast are the two leading commercially available programs for simulating Lost Foam casting. ProCast assumes the foam is converted to gas at the metal-foam interface and recently incorporated gas escape through the coating and sand. Flow-3D considers transient liquid formation but does not provide for gas escape or pressure in the pyrolysis zone. Flow 3D does consider heat transfer at the liquid metal surface and tracks the metal free surface.

The features of flow and fill have been examined in a study of a V6 engine block. The results predicted areas of defect formation, but some adjustments of the heat transfer coefficient were necessary to provide metal velocities that matched experimental values.

1.2.2 Development of Physical Model

Previous research has shown that patterns are degraded into gas and liquid components in a kinetic zone between the metal front and the receding pattern. The air in the pattern and the pyrolysis gases were thought to exit the casting cavity through the coating in the kinetic zone. The remaining liquid components were thought to flow into the metal/coating interface by a combination of wetting, wicking and pressure driven flow. These liquid components were heated by the metal and converted to gas which passed into the sand after the metal front had passed.

Burke, Gustafson and Zhao proposed an alternate mechanism where the liquid pyrolysis products trapped between the metal and coating formed liquid carbonaceous islands that degrade to gas which flows through the coating. Depending on local temperatures and pressures, the gas could break the metal surface tension and enter the metal to produce porosity and folds. Heat transfer conditions at the metal/coating interface favor this mechanism. The liquid does not initially wet the coating, as previously assumed, but instead slowly degrades into gas in contact with the hot metal. Polystyrene vaporization creates an insulating gas film around the pools which keeps the polymer at a relatively low temperature (180-400°C). The area covered by the pools decreases with time (or distance from the metal front) as the polymer degrades.

The vaporized liquid either passes through the coating or enters the metal, depending on local pressures. EPS degradation products and air from the pattern escape from regions between the metal and the coating through areas not covered by the liquid pools of pyrolysis products.

The proposed escape path for gases was challenged since this path did not accommodate pattern permeability. Patterns segments were pushed against heated blocks at typical aluminum temperatures and then quenched in water. A surface layer of liquid polystyrene with multiple holes was found on the degraded surface, followed by a layer of collapsed beads and then the virgin pattern beads. These observations indicate that the gap between the metal front and liquid layer is functioning as a heat transfer gap, and the gap behind the liquid layer is functioning as a gas exit path. The holes in the liquid layer allow gas access to the pattern. These results have been incorporated into the physical model of metal/pattern exchange.

The transfer of the gaseous pyrolysis products from the casting cavity during metal filling was examined using a screen window on the wall of a casting flask. Considerable amounts of gas were visible at and behind the advancing metal front. The movement of liquid pyrolysis products was examined by pouring onto the foam patterns. Bubbles containing gaseous and/or liquid pyrolysis products floated through the metal and burst at the top. These observations indicate that entrapment of gaseous and liquid pyrolysis products occurs during and after metal filling occurs.

1.2.3 Development of Algorithms

Data was needed on the size of the kinetic zone (KZ) between molten metal and receding patterns, the temperature distribution in this zone, and the viscosity of gaseous and liquid degradation products. These data cannot be directly measured so a heat and mass transfer model was developed. The model was based on principles of mass/heat transfer, lubrication theories, experimental pattern degradation data, and video recordings of pyrolysis experiments.

The KZ was assumed to have a uniform thickness and to consist of a mixture of liquid and gaseous degradation products with average and uniform viscosity, heat capacity, and thermal conductivity. The temperature in the KZ was assumed to vary from the heater temperature to the EPS “melting” temperature (150°C). Heat transfer in the KZ was assumed to occur by conduction, convection, and radiation. The model used data including heater power density, gas fraction, and resistance pressure.

The KZ parameters were calculated for aluminum casting conditions using degradation data for 25 kg/m^3 EPS developed for the range of 600-790°C at foam recession rates of 1, 3, and 4.5 cm/s. At recession rates of 3 cm/s and 4.5 cm/s, the KZ thickness did not vary with the heater temperature and was estimated at 0.06 mm and 0.04 mm, respectively.

At a recession rate of 1 cm/s, the predicted KZ thickness increased from 0.16 to 0.2 mm as the heater temperature increased from 600°C to 790°C. The average KZ temperature did not depend on the recession rate and was estimated to be between 335°C and 405°C for a heater temperature range of 600-790°C.

The average density of the mixture of gaseous and liquid pyrolysis products in the KZ was calculated using the ideal gas law and the rule of mixtures. In the heater temperature range of 600-790°C, the KZ density was estimated at 12-10.7 kg/m^3 at a recession velocity of 1 cm/s, 15.9-11.2 kg/m^3 at a recession velocity of 3 cm/s, and 23.5-11.9 kg/m^3 at a recession velocity of 4.5 cm/s. The estimated viscosity of the mixture of the liquid and gaseous degradation products decreased exponentially from about 0.02 to 0.0013 poise as the average KZ temperature increased from 330°C to 405°C. The recession velocity was not affected by the viscosity.

The model developed through data must be extended to describe heat/mass transfer in the KZ under casting conditions. The main issues include: (a) the effect of pattern properties and geometry on the metal front shape and (b) the escape of pyrolysis products through the coating.

1.2.4 Computational Model

Flow Science incorporated the physical model to predict defect sites in a box pattern and a marine engine block. The simulations used UAB velocity data to calculate the heat transfer coefficients, and predicted defect locations agreed well with the experimentally determined locations. Although progress is being made, it is still necessary to have correct heat transfer coefficients as a function of metal velocity.

UES Software has updated the Pro-CAST Lost Foam module to include the effects of gas pressure produced by pattern degradation; however, the values of permeability are artificially high. Although the improvement is significant, additional development remains to track liquid prolysis products.

FLOW-3D® has demonstrated their capability to locate probable defects in castings, and provide insight into the origin of defects (see Fig. 6). This information can then be used to make process improvements. For example, the computational model suggested that a certain gate modification would reduce defect formation. This was indeed found to be the case.

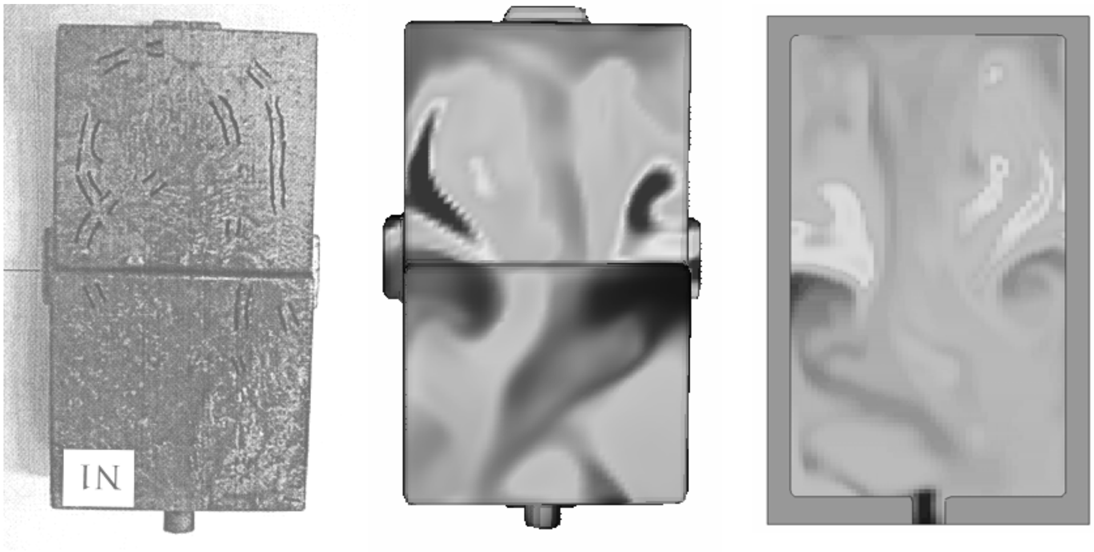

Figure 6. Comparison between experimentally observed defects (left), computational predictions in bottom (middle) and slightly deeper into bottom surface (right). Box pattern was used for this work.

New capabilities were incorporated into FLOW-3D® to enable users to describe pattern density gradients. The utility of the predictions was evaluated using instrumented castings and x-ray examinations of both simple and complex castings.

The model predicted reduced porosity in a new engine block design, and correctly predicted reduced porosity with a gate change. It was also found that the metal temperature distribution at the end of the mold filling was not uniform, and this had an important effect on shrinkage. The FLOW-3D®

shrinkage model predicted the general location of the porosity, but the location was biased slightly toward the cylinder walls.

1.2.5 Validation with Real Time X-Ray

Real time x-ray results indicated that local pattern permeability had an important effect on the shape and velocity of the metal front. High pattern permeability results in higher metal front velocities. Pattern permeability differences were simulated by assigning pattern densities values to different pattern regions based on permeability measurements. The working hypothesis was that higher permeability regions would have higher foam replacement rates. By segmenting patterns into regions with density inversely related to permeability, the dynamics of pattern replacement were simulated without multi-phase modeling.

Simulation results gave a much better correlation with metal front shapes when permeability was incorporated. Moreover, when an inverse exponential functionality was used between density and permeability, the metal front shape was nearly identical to that observed in x-ray observations. The correlations have prompted the use of this modeling technique to address production casting issues.

2. Casting Dimensional Accuracy

The objective of this task was to identify sources of casting distortion. These studies included dimensional studies on blown patterns, glued pattern assemblies, coated and dried assemblies, and distortion caused by the compaction and pouring processes. Control measures were implemented in the foundries.

2.1 Sources of casting Distortion

2.1.1 Case Study 1: long pipe

An opportunity arose to study distortion of eight foot tall flasks. These flasks amplify pattern distortion because of the pattern length. Pipe extensions ranging from 3 to 6 feet long are cast in a four-on configuration. Molds are prepared on a vertical compactor. Some bending and length reduction were being experienced. Experimental work identified bending to a result of non-uniform sand filling in and around the pipe extensions. The sand force on the outside of the pipe pattern caused the pattern to bend towards the unsupported interior. Since the pattern was unsupported at the top, the cumulative effect was a distorted pattern and casting. The distortion was minimized by masking the sand rain gate to produce uniform filling in and around the pattern. Additional dimensional accuracy was obtained by suspending the cluster from the sand hopper.

2.1.2 Case Study 2: Valve body

The distortion associated with the production of a valve was also conducted by applying strain gages to patterns, calibrating the strain gages, and measuring the deformation during sand filling and compaction. The experimental set up is shown in Fig.7, and a typical pattern distortion curve is demonstrated in Fig.8. The data indicated that sand was being compacted around the valve before the interior cavities were filled. This caused lateral movement of the pattern walls toward the unsupported interior. The distortion could be significantly reduced by simply rotating the valves 90 degrees in the flask.

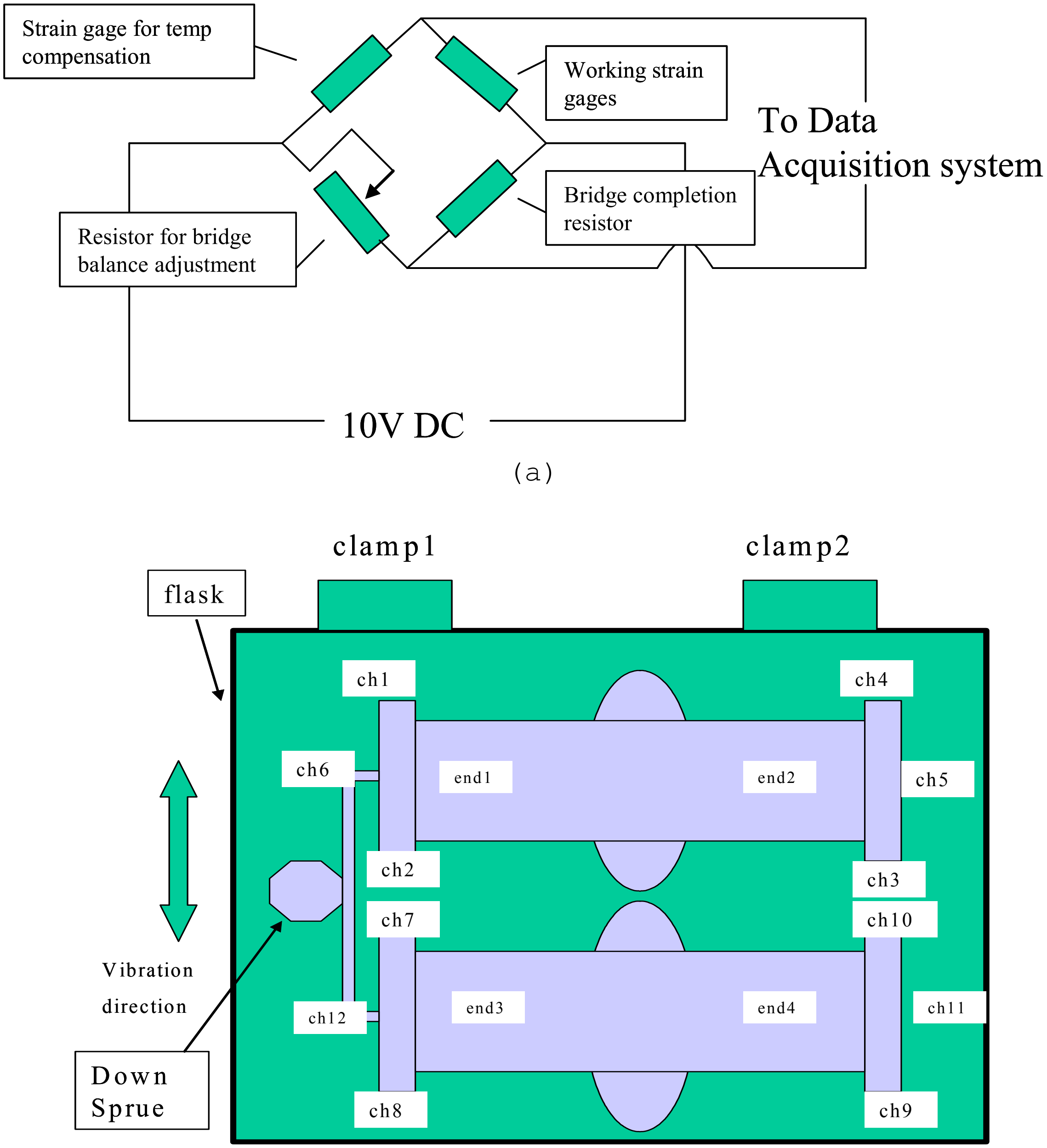
Strain gage for temp compensation
Working strain gages
To Data Acquisition system
Bridge completion resistor
Resistor for bridge balance adjustment
10V DC
clamp1
clamp2
flask
ch1
ch4
ch6
end1
end2
ch5
ch2
ch3
ch7
ch10
Vibration direction
end3
end4
ch11
ch12
Down Sprue
ch8
ch9

(a)

(b)

Fig.7. Experiment Set-up for 6in Valve. (a) Electric circuit of the testing apparatus. There are 12 channels in the apparatus. Each channel has the same circuit. (b) Location of the strain gages.

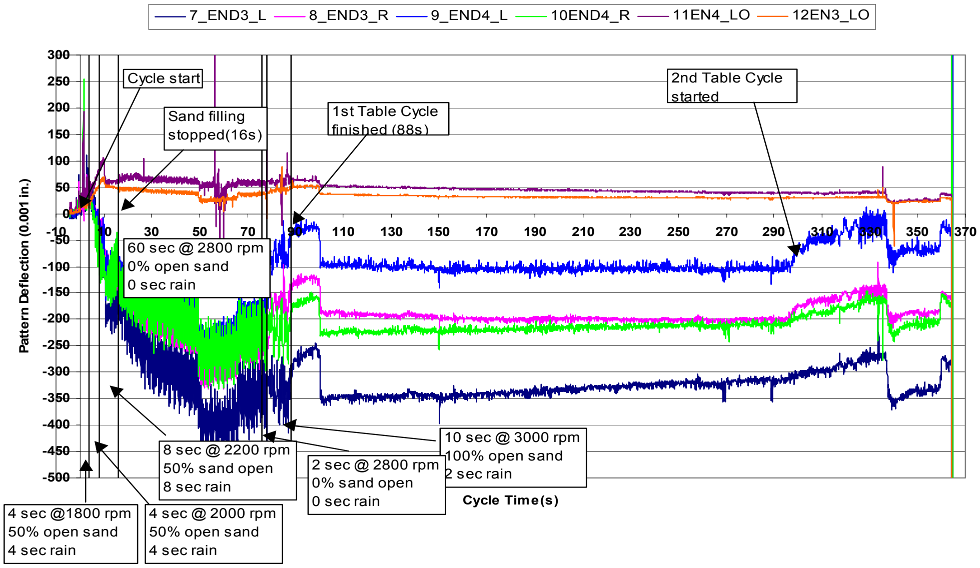

Fig.8. Foam pattern dimensional change during sand filling and compaction.

2.1.3 Sources of casting distortion

Table acceleration and sand angularity were two parameters having a significant effect on pattern distortion during flask filling and compaction. Higher table accelerations and more angular sands produced more distortion with constant table accelerations.

Sand thermal expansion has also been identified as an important factor. Silica sand, which has a phase change around 1000°F, expands more than other sands such as olivine, chromite, and synthetic mullite. Synthetic mullite has a low coefficient of thermal expansion and rounded grains that flow easier at low table accelerations. Several foundries are now using synthetic mullite to improve casting precision.

3. Pattern Production

The objective of this effort was to understand parameters that control foam pattern dimensional stability including the effects of pre-expansion, bead conditioning, blowing parameters, steaming, and pattern aging effects. A data base containing properties of polymeric materials currently used in Lost Foam patterns was also developed. These properties are required for computational codes to accurately describe the metal/ pattern replacement process and predict defect formation. Another part of this work was to understand the role of vented and ventless pattern tooling on the bead filling and steaming of patterns.

3.1 Pattern Bead Properties

3.1.1 Properties of Raw Beads

Research during an earlier phase determined the specific heat and degradation energy of Polystyrene (PS), Polymethylmethacralate (PMMA) CoPolymer (a blend of PS and PMMA)using Thermogravimetric Analysis (TGA), and Differential Scanning Calorimetry (DSC). The differences in properties were small, and no further efforts with DSC or TGA are anticipated because the pyrolysis properties are better measured using procedures described previously in section 1.1, pattern material degradation properties database.

3.1.2 Pattern Density Measurement with Dielectric Sensors

A new approach to nondestructive pattern density measurements, based on a dielectric constant sensor, was evaluated. The dielectric properties of foam samples were determined after the samples were soaked in olive oil to fill the open pores. The bulk density and open porosity was then measured using a buoyancy technique.

A linear relation was found between the dielectric constant, the dielectric values from oil saturated samples and the open porosity values. Both correlations agreed with a theoretical model. In-plant measurements on patterns, as they were removed from the molding machine, indicated that this method is an effective on-line process control tool. Development work is needed in more plants to confirm its utility.

3.1.3 Pattern permeability

3.1.3.1 Apparatus

A permeability apparatus (see Fig.9) has been developed to measure pattern permeability. The degree of fusion, which is reflected by permeability measurements, is a major factor affecting casting defect formation. This permeability technique uses a vacuum source with a suction cup applied to patterns. Pattern permeability can vary by a factor of 100 depending on the degree of fusion, and the pattern permeability is as high or higher than coatings used to make aluminum castings. A 'threshold' value of the steaming pressure has been found that produces a fused pattern surface with low permeability. This discovery led to a better understanding of the escape path for gas during pattern decomposition. A portable version of this apparatus has been developed for use at or near pattern blowing machines. The repeatability of this apparatus is demonstrated in Fig.10. The Pattern Permeability Apparatus is currently being evaluated in a sponsor foundry to improve pattern consistency and casting quality.

3.1.3.2 Pattern Thickness and Degree of Fusion

A computational model of gas flow into the suction cup was developed to understand the effects of pattern thickness and degree of fusion. Permeability constants for low and normally fused patterns were used in the calculations. Air compressibility and inertial flow effects were neglected for simplicity. Air flow was modeled using uncoated patterns with thicknesses of 0.4 cm, 0.8 cm, 1.6 cm, and 2.4 cm. The suction cup gaskets dimensions were 1.27 cm ID and 0.48 cm wide. The vacuum level was - 2 psi. Uniform and non-uniform parabolic pattern permeability variations through the plate thickness were considered. Patterns with a non-uniform permeability were described by the ratio of the pattern center to surface permeability constants. Patterns with permeability constant ratios of 2, 5, and 10 were modeled. Permeability constants (Bo) of 10^{-8} and 10^{-9} cm^2 were used in calculations.

Pattern thickness had a significant effect on the air flow rates, and flow rates through the cup decreased as the plate thickness increased. When the permeability was uniform with a value of 10^{-8} the normalized flow rates decreased from 28.5 $cm^3/(cm^2.s)$ to 19 $cm^3/(cm^2.s)$ as plate thickness increased from 0.4 cm to 2.4 cm. When patterns had the same thickness but a non-uniform permeability, the flow rates decreased from 24.2-27.2 cm^3/cm^2s to 10.3-15 cm^3/cm^2s, depending on the center-to-surface permeability ratio.

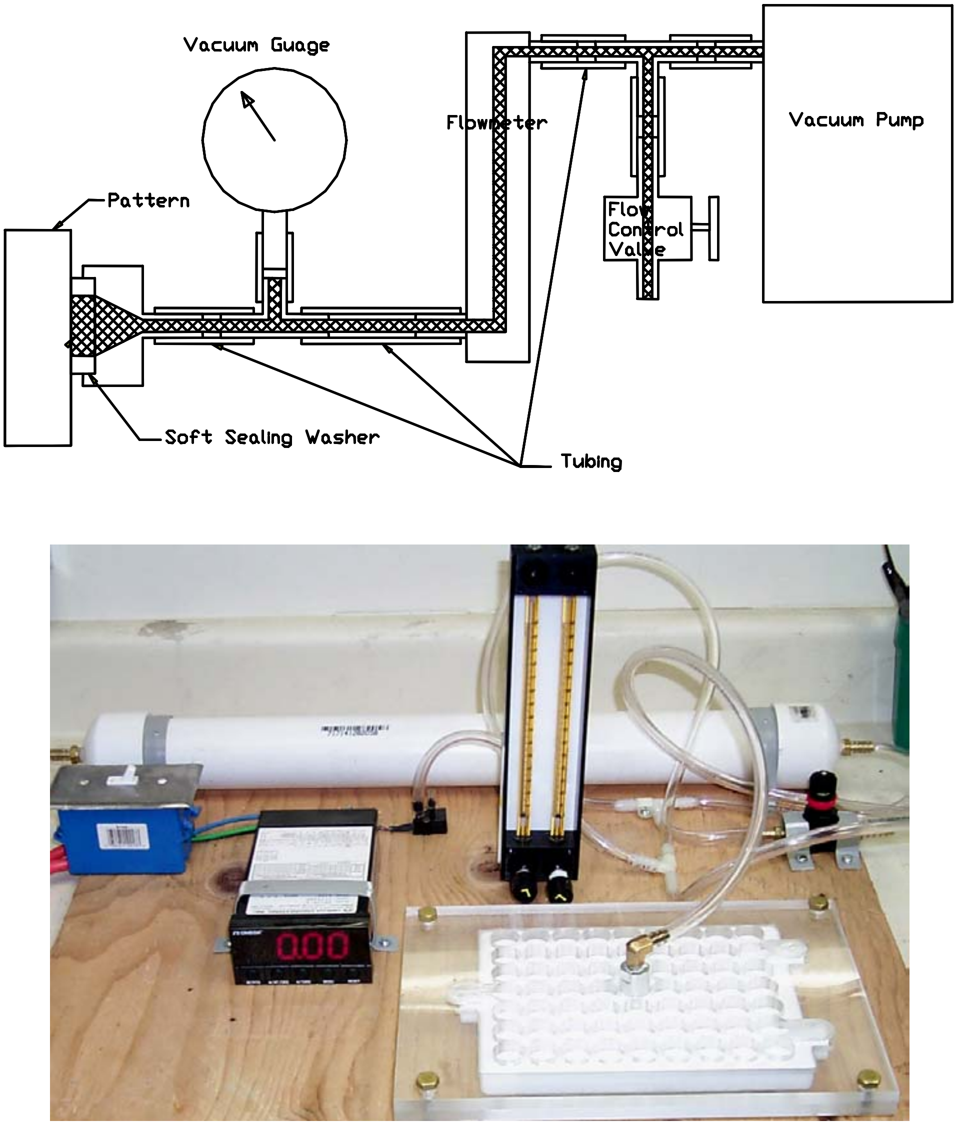

Fig.9. Apparatus for Measuring Pattern Permeability

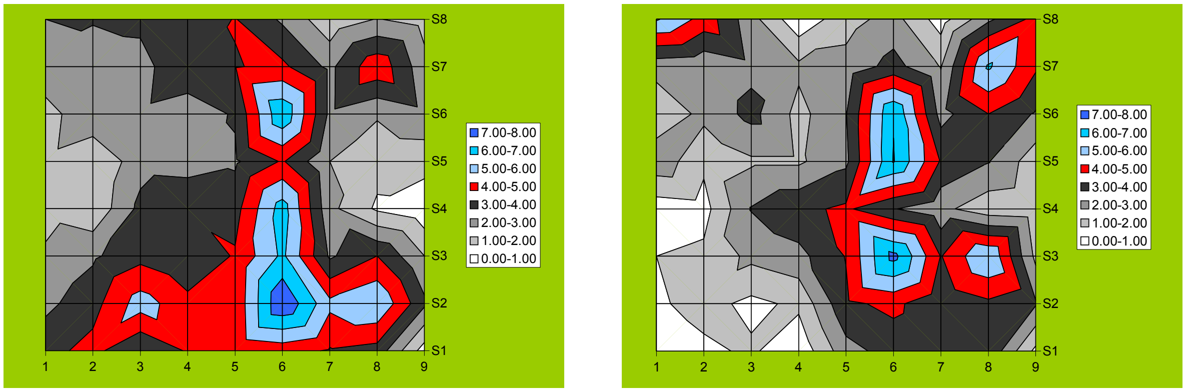

Fig.10. Repeatability of foam pattern permeability.

Air flow through the rear of the plate accounted for about 90% of the total flow through the cup in plates having a thickness of 0.4 cm. The fraction of air coming through the rear side of the plate decreased to 26-40% as the plate thickness increased to 2.4 cm. Most of the flow occurred within 2-3 mm near the boundary of the gaskets on the front pattern face.

The measured air flow rates through patterns having different thicknesses cannot be compared. The utility of this apparatus will be realized by comparing air flow rates at specific locations on production patterns.

3.1.3.3 Pattern Permeability, Metal Filling and Casting Quality

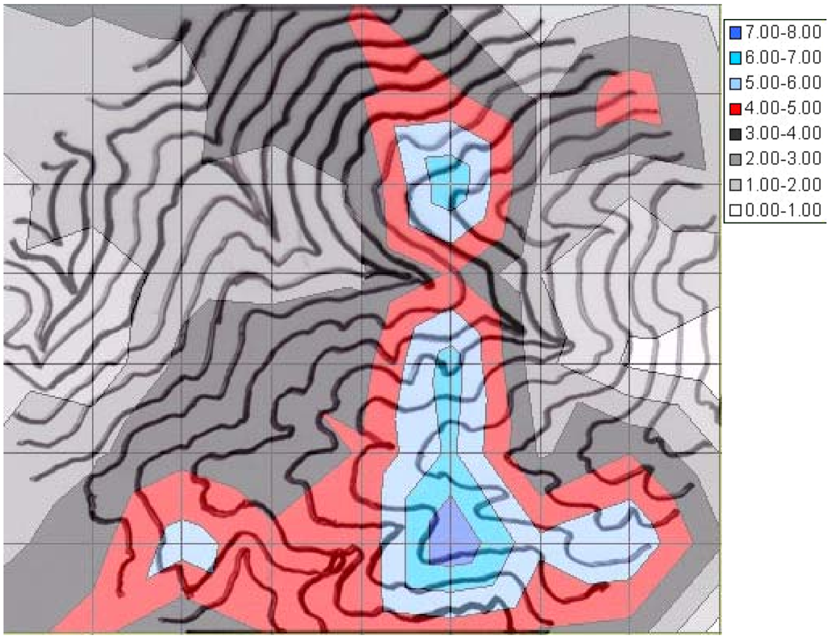

Fig. 11. Overlay of metal filling profile and foam pattern permeability showing effect of pattern permeability on metal filling behavior. The interval of the metal filling profile is 0.4 second, and the unit of the pattern permeability is: $cm^3/(cm^2.s)$

Real time x-ray results have shown that pattern permeability differences have a dramatic effect on the shape and velocity of the metal front during pattern replacement (see Fig. 11). Locally high permeability values increase metal front velocities which results in multiple metal fronts that converge to produce carbonaceous fold defects.

3.1.3.4 Pattern Permeability Threshold

A threshold gas flow rate that causes melt front instability was defined to develop permeability acceptance criteria. Metal filling profiles from different patterns were overlaid, and the minimum permeability value affecting filling behavior was found to be about 1.0-cc/sec-cm^2 in 10mm thick plates.

Work was continued on plates having different thickness values and on commercial patterns. High permeability (low fusion) results in erratic metal fronts, higher metal velocities, and a higher probability of folds forming. Local pattern air flow rates above 0.5 cc/sec.-cm^2 lead to perturbations in metal front shapes that could produce folds at merging metal fronts. The uniformity of local air flow rates may be more important than the absolute values.

3.1.4 Computational Models for Bead Filling and Steaming

Arena-flow LLC., took the lead in this task. Arena-flow developed software, Arena-flow-EPS, to simulate the bead blowing process and assist tool design and blowing parameter selection.

The model was improved and tested at three sites: UAB, Arena-flow LLC., and General Motors. Arena-flow was responsible for developing physical and mathematical models of bead packing and local density gradients. Twenty-five (25) foam patterns were selected and maps of the permeability were made. These the patterns were supplied to Walford Technologies for density mapping using an X-Ray scan technique. These data were given to Arena-flow to further develop and validate blowing and steaming models.

When the improvements were incorporated, Arena-flow-EPS was successfully used for production application. A loosely packed low density area in the combustion chamber area of cylinder head pattern was predicted. Based on the modeling results, the process parameters were adjusted, and the defect area in the foam pattern was eliminated. However, modeling failed to simulate two of the most important pattern properties – pattern permeability and density gradients.

3.2 Pattern Tooling

3.2.1 Pattern Cooling and Density

It has been found that the wall thickness of a pattern tool has little effect on the rate of pattern cooling. It was originally thought that density gradients within a pattern were due to uneven cooling across a section, and that changing the tool wall thickness could eliminate the gradients. Cooling relies on conduction, and the conductivity of EPS is four orders of magnitude lower than the aluminum mold. Thus, no matter how quickly the mold is cooled, the pattern can only cool at a rate permitted by conduction within the pattern. Computer models incorporating an aluminum mold and solid foam patterns have proven this to be true. Water vapor in the pattern is the main heat conductor within a pattern.

Additional studies were made to simulate cooling during pattern molding. The open porosity and water content were varied to determine the effects on cooling rates. The resulting data were inconsistent with experimental data from molding experiments. The models did show, however, that patterns with higher open porosity cooled quicker because of the higher thermal conductivity below 100° C. This was attributed to more entrapped water in these foams.

3.2.2 Tooling Types and Permeability

Vented and ventless tools provide very different bead filling and steam boundary conditions. A series of 10mm thick plate patterns was made with both low and normal degrees of fusion and blown in both vented and ventless tools. The two types of tools produces significant differences in metal velocities, metal front shape and defect occurrence.

Patterns produced in ventless tools have higher permeability compared to those molded in vented tools. Lower permeability gradients, i.e. more uniform patterns, were observed in patterns produced in vented tools, and the back sides of the patterns had relatively uniform and lower permeability values. Higher permeability gradients were found in patterns molded in ventless tools.

The distribution of high permeability regions was compared. Most of the high permeability regions were repeatable from pattern to pattern. However, the high permeability islands on the front and back faces of the patterns prepared in vented tools were not symmetrical. The patterns blown in ventless tools were symmetrical on both pattern surfaces. This indicates that vents change the bead filling and steaming behavior.

The distribution of high permeability regions in patterns having high and low degrees of fusion molded by the same tool was different. Only one high permeability region appeared on both of the high and low fusion patterns, while many others only show up either in low fusion or in high fusion foam patterns produced in vented tools. One explanation might be that longer or higher pressure steaming not only cured the high permeability area, but also produced new high permeability regions by moving or collapsing the beads. However, in ventless tools, most of the high permeability regions seen on low fusion patterns are also seen on high fusion patterns. This could be explained by: 1) The degree of fusion in “high” fusion patterns is not as high as expected; 2) Bead filling may be basic cause of the permeability islands or; 3) Bead movement is limited during steaming. Additional study is required to understand the controlling mechanism.

3.2.3 Filling and Bead Arrangement

The working hypothesis about the location of density gradients is that the gradients develop when the beads are blown by the fill guns. Beads in a pyramidal stacking arrangement with a density of 1.4 pcf can theoretically have a density as low as 1.0 pcf if stacked in a simple cubic arrangement. If the stacking arrangement could be controlled, the density gradients might be also controlled.

It had previously been thought that the prepuff density and the bead filling process controlled the pattern density. However, this is only true if the bead packing arrangement is consistent. A literature review showed that inconsistent bead packing could produce areas with dramatically different densities and void fractions (open porosity/permeability). More studies is required to understand bead filling and arrangement during pattern molding.

3.2.4 Pattern Molding Parameters

3.2.4.1 Experimental approach

A full factorial matrix was conducted including: pre-expanded bead density, pre-expanded bead volatile content, steaming time, steaming pressure, vacuum assisted cooling, and bead filling pressure. The residual volatiles consist of pentane and moisture at the time of molding. The volatile content was controlled by letting the beads age from 24 to 72 hours. The pre-expanded bead density was changed in the pre-expander by varying the steaming time.

Flange tooling was instrumented with thermocouples and pressure transducers to record events in the molding cycle. The temperature of the tool wall, center of the pattern cross-section, and the surface of the pattern was recorded. The pressures inside the steam chest and inside the pattern cavity were also recorded.

The degree of fusion and pattern density were measured using a low power x-ray absorption technique by Industrial Analytics Corporation. The fusion measurement produces a qualitative number that is a function of the pattern surface and pattern shape. The open porosity, density, and density gradient of patterns were measured using the olive oil absorption technique.

3.2.4.2 Degree of pattern fusion

The fusion index varies as a function of the pre-expanded bead density and the bead volatile content, with the volatile content having the greatest effect. The cross-sectional density gradient was affected by the volatiles, pre-expanded bead density, and the location in the pattern. The pattern volatile content also had the largest effect on the density gradient.

The fusion index and the cross-sectional density gradient correlates with higher values associated with higher cross-sectional density gradients. Open porosity was related only to the fill gun location.

Higher bead densities and/or bead volatile contents increased the fusion index and the cross-sectional density gradient. The degree of pattern fusion and the cross-sectional density gradient, based on x-ray measurements, were especially sensitive to residual volatiles in pre-expanded beads. The fact that the fusion index and density gradient were both affected by volatile content indicates that the driving forces behind fusion and density gradients could be the same.

3.2.4.3 Open porosity

Patterns that were steamed with the highest temperatures and times had low values of open porosity and did not appear to be substantially affected by other molding variables. Patterns that were steamed at lower temperatures and times had higher values of open porosity and were affected by other molding variables. Open porosity varied with the time that the pattern was above the Glass Transition Temperature (100°C). The open porosity decreased with time until after about 25 seconds. Some increase then occurred, perhaps because of bead collapse.

SEM analysis was made on patterns suspected to have typical open porosity and open porosity caused by bead collapse. The patterns suspected to have bead collapse had many holes in the bead cell skin. These holes would cause the measured open porosity to be higher because of olive oil penetration. By comparison, the remaining patterns had very few holes in the beads.

The cross-sectional density gradient increased as the time above 100°C increased and as the steam pressure increased. The gradient was most sensitive to the molding variables at intermediate power levels.

3.2.4.4 Density Gradient

Cross-sectional density gradients ranged from 1.0 (no gradient) to 1.2, a substantial gradient. The gradient increased as the time above 100°C increased and as the pressure on the pattern increased. The gradient was most sensitive to the molding variables at intermediate power levels.

The density values measured using two techniques had a correlation coefficient of 0.94, and the open porosity measurements had a correlation coefficient of 0.54. A linear trend existed between the two porosity values with the x-ray technique providing a lower average values compared to oil immersion.

Higher pressures in the pattern and the time that the pattern was above 100°C affected the density gradient proportionally. Sections have larger gradients if the pattern remains above the glass transition temperature (100°C) for longer periods of time.

3.2.4.5 Foam pattern temperature and pressure

The patterns were classified according to the steaming energy applied: low, medium/low, medium/high, and high. The steaming energy associated with the low value was 1.1 bars of steam pressure for 6 seconds; the medium/low values were 1.6 bars for 6 seconds; the medium/high values were 1.1 bars for 10 seconds, and high values were 1.6 bars for 10 seconds. In general, higher power inputs produced larger temperature gradients and higher cavity pressures. The use of vacuum-assisted cooling and the bead volatile content had the most significant effect on the temperature and pressure.

Thermocouple and pressure data from molding experiments generally supported the working hypothesis. As the input energy was increased, the temperature and pressure gradient in the pattern increased. At both the lowest and the highest power input values, the pressures and temperatures were not substantially affected by the volatile content. The temperature and pressure readings were sensitive to all molding variables at intermediate power input values.

The temperature and pressure data proved that pattern properties are sensitive to the molding parameters. At high power input values, the process was robust, and the steam cycle overwhelmed all other variables. At low power values, variations in the bead volatile content had a much larger effect.

3.2.5 Pattern Properties and Casting Quality

It was hypothesized that an arrow-shaped metal front would be the most desirable during pattern replacement. Such a front shape should help drive the liquid by-products from the cavity. A large cross-sectional density gradient and/or a pattern open porosity should encourage the arrow shape. The density gradient was produced during the cooling cycle where the center of foam pattern continued to expand while expansion in the surface layers slowed because of the cooling.

Hopper first reported a relationship between bead fusion and casting defects (UAB – 2001/2002). The degree of pattern fusion was controlled by the bead exposure time above the glass transition temperature. He also found a relationship between the degree of bead fusion and pattern open porosity. Casting results indicated that casting defects were more frequently associated with higher levels of pattern open porosity.

Casting experiments were conducted with patterns having wide variations in bead density, steaming pressure, and steaming time. These variations produced large differences in open porosity and cross-sectional density gradients.

Two mechanisms were found to control the metal fill velocity. The metal front velocity for 1.2 pcf patterns appeared to be controlled by density gradients while at higher pattern densities, the velocity was controlled by pattern open porosity. The velocity at the lower density appears to be controlled by removal of liquid pyrolysis products, and the velocity at higher densities by gaseous by-product removal. A large cross-sectional density gradient produced a relatively flat metal front. Patterns with the smallest density gradients produced arrow-shaped metal fronts. These results proved the hypothesis to be wrong.

Defect occurrence was not sensitive to the metal front shape. Patterns that produced a relatively flat front produced the fewest number of folds. Patterns having a cross-sectional density gradient and high open porosity produced a metal velocity of 1.8 cm/sec, a nearly ideal fill velocity. In general, patterns producing higher or lower velocities produced more casting defects. Bead collapse may have been responsible for the defect reduction. Ruptured cells may collapse faster and increase the removal of liquid pyrolysis products, thus reducing fold defects.

3.2.6 Pattern Quality Control Manual

A Pattern Quality Manual was developed and distributed to the sponsors. The manual provides procedures for measuring pattern density, open porosity, and volatiles as well as techniques for measuring pre-expanded bead density, and volatile contents. Equipment, procedures, and data processing techniques are described.

4. Pattern Materials and Processes

The objective of this task was to improve the pattern degradation properties and reduce casting defects. Degradation of EPS, Co-polymer and PMMA were addressed in Subtask 1.1. The property data has helped 1) understand current pattern materials, and 2) to identify alternate materials. EPS having a range of molecular weights was included.

4.1 Improved Pattern Materials

Development of new polymers is a lengthy process. The costs far exceed the potential return on investment for the limited lost foam market, and as a consequence, new pattern materials have not been developed. The approach taken in this project is that efforts should concentrate on enhancing currently available pattern materials. Developing a pattern precoat was the first effort conducted.

4.1.1 Foam Pattern Pre-coat

The use of a pre-coat applied to flange patterns, prior to the refractory coating, was found to reduce surface fold defects. Confirmation experiments were performed using a box pattern. The box pattern is complex, and provides a variety of metal flow characteristics. Eight castings were poured, four of which had been pre-coated with a proprietary material.

There was an 82% decrease in the number of folds and a reduction in average fold length of 42%, although some blisters and cold shuts occurred. The mechanism for fold defect reduction is not known, but it appears that the fill velocity is lower and more uniform. This infers that the pre-coat reduced the metal velocity by sealing the pattern surface porosity.

4.1.2 Development of “No Fold” Beads

A bromine additive was added to T180 beads to produce a T185 “no fold” bead stock, and the effects of pattern density, fusion, and coating type were examined. Castings poured using T185 beads replaced the pattern more slowly, and exhibited fewer and smaller defects (see Fig. 12). The use of a low permeability/high liquid absorption coating also decreased the metal velocity and reduced the number of defects.

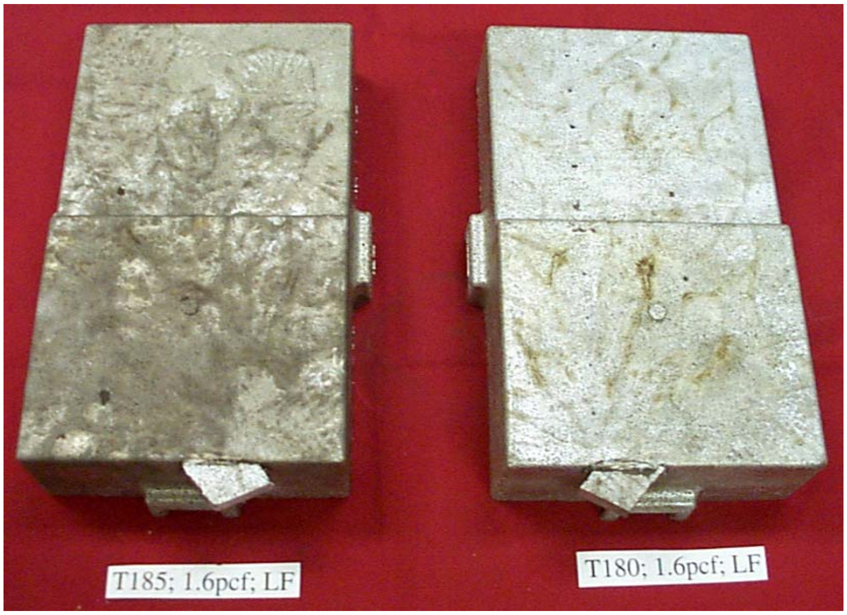

Fig. 12. Comparison of the resulting casting surface between the T180 and T185 patterns. T180 = no additive foam beads, T185 = with additives foam beads.

The difference in metal velocity as high density T180 and T185 patterns were replaced was negligible. However, the degree of pattern fusion had a significant effect on defect size with T180 but not with T185 beads.

4.1.3 Evaluation of Alternative Foam Materials – Polyurethane

Pattern degradation research done in Subtask 1.1 indicated that the liquid pyrolysis products accounted for 60-70% of the pattern weight at aluminum pouring temperatures and 30-40% at iron pouring temperatures. Liquid products are the root cause of most casting defects. The ultimate solution to eliminate defects is to develop patterns that degrade entirely into gaseous products.

Three types of Polyurethane (PU) foam, identified as High Functionality, Low Functionality, and Taztol were evaluated as alternative pattern materials. PU foam patterns produced smoother surfaces than EPS which would benefit fatigue properties. With the exception of the Taztol foam, the PU foams performed satisfactorily during coating, drying, compaction and pouring. The Taztol foam collapsed as the coating was dried. Both aluminum and iron castings were poured, but quality of the castings was unacceptable because the foam density was too high. A lower density should provide a significant improvement in casting quality.

A comparison of PU and EPS foams indicates that PU foam might be suitable if the material has sufficient stiffness. However, the literature indicates that CO and HCN are produced during pyrolysis, and this could be objectionable in production environments.

4.1.4 Evaluation of Alternative Foam Materials - PMMA

Several observations were made based on pattern degradation in Section 1.1). First, EPS degrades to about 20 – 30 % gas (70 – 80 % liquid) at aluminum pouring temperatures while PMMA degrades to about 70 – 80 % gas (20 – 30 % liquid). Since liquid pyrolysis products are the root cause of many casting defects, PMMA could be a candidate pattern material.

PMMA patters were prepared using a box pattern, coated and poured through different sprues. Casting surfaces were cleaner than those poured with EPS patterns; however a significant number of folds were formed. Castings poured with EPS patterns using a high permeability coating with foam sprues and castings produced with low permeability coatings and ceramic sprues produced some fold defects.

Castings poured using PMMA patterns, high permeability coatings and ceramic sprues and those poured using low permeability coatings and foam sprues were worse. The combination of a high permeable coating and ceramic sprues probably produced turbulent metal flow and folds, while low permeability coatings and foam sprues reduced the velocity and the formation of fold defects.

Metal replacement of PMMA patterns was examined using the real time X-Ray system. Metal bubbling was observed at the metal front. The gas reduced the pattern replacement rate, and some parts did not fill completely. This study also provided information about mass transfer during foam replacement.

A similar study was made using 10mm thick plate patterns prepared with PMMA and EPS. There was a significant increase in the number of folds with PMMA compared to EPS patterns. Auger analysis found carbon and high oxygen concentrations in folds associated with PMMA patterns. The oxygen present in PMMA apparently aggravated fold formation.

4.2 Improved Pattern Degradation Process

4.2.1 Pattern Additives

Some additives to foam patterns show promise for facilitating polymer degradation. Several experiments were conducted to explore their effects. Beads with additives were prepared by Styrochem, blown, coated, and castings poured. The results were presented in section 1.1.3.3.

4.2.2 Coating Additives

The addition of tri-calcium-phosphate (TCP) to coatings has shown promise in reducing pyrolysis residue on aluminum castings. Although the mechanism is not understood, the compound appears to release oxygen to accelerate pyrolysis.

TCP additions did not eliminate surface pyrolysis traces, but they were reduced and the coatings pealed cleanly from the casting surfaces. TCP significantly reduced the lustrous carbon defects on iron castings. The literature suggests that TCP may react with carbon to remove it from the casting surface.

4.2.3 Effects of Pouring Atmosphere

A technique to pyrolize patterns at high heating rates was developed by Walford Technology. This technique uses a laser spot as a heat source and an infrared camera to monitor pattern degradation. Pyrolysis is done in a sealed container, and pyrolysis products can be collected for analysis. Using this technique, T185 no fold bead was found to disintegrate faster, and the presence of Helium significantly increased the rate of degradation.

The possibility of introducing some helium into patterns was also examined. Reducing the air contained in beads might reduce the severity of oxide films in castings. The air content in foams can be reduced by vacuum treatment and infiltration with an inert gas. However, the patterns should be used quickly to prevent air reentry. The kinetics of air reentry and the potential benefits of this approach are not yet established.

Walford Technology has questioned whether pattern fusion rather than permeability might be critical feature affecting the production of good castings. This hypothesis was explored using radiation imaging where patterns were laser heated and the response recorded with an infra-red camera. The internal bead fusion correlated with oil permeability data. Highly fused regions of patterns had higher radiation heat transfer factors compared to regions having a lower degree of fusion. This issue requires additional study.

4.2.4 Pattern Degradation Energy

A study of EPS pattern degradation between 300 ^{0}C and 700 ^{0}C was conducted to separate pattern melting and gas formation effects. The Pattern Pyrolysis Apparatus (see section 1.1.1) was used with a pre-heated block to simulate molten metal. A constant pressure of 1.5 psi drove patterns into the block, and pressure and displacement were recorded. The pattern recession velocity was a linear function of metal temperature up to 480^{0}C. The velocity decreased over a short temperature interval and then became linear at about 500 ^{0}C. These results indicate that very little pyrolysis occurs below 480 ^{0}C, and at these low temperatures, patterns are degraded primarily by melting. Above 480^{0}C, pyrolysis occurs and a gas layer between the metal and receding pattern reduces the replacement velocity because of the insulating gas effect on heat transfer.

5 Coating Control and Vacuum Assist

The objective of this investigation was to improve the procedures for measuring permeability and liquid absorption of coatings. A faster response to changes on the foundry floor was needed along with some improvements in precision. Another objective was to understand the relationship between coating permeability and extend lost foam casting technology to produce steel castings.

5.1 Coating Quality Control

5.1.1 Coating Control – Case Study

The Coating Quality Control Procedures were used at a foundry producing aluminum engines. Inconsistent permeability data was traced to inconsistent drying procedures.

5.1.2 Correlation between UAB and GM Coating Permeability Procedures

A correlation was developed between the UAB permeability values and the values obtained by GM. This correlation was necessary to assist UAB personnel in troubleshooting efforts. Correlations between the values were examined using ten typical coatings with permeabilities covering the range commercially used for producing both aluminum and iron castings. Although theory predicts a linear relationship between data obtained with both techniques, a linear relationship was not obtained.

It was found that the GM procedure measures coating permeability as it is influenced by both permeability and coating thickness as affected by viscosity. The UAB technique measures permeability in a way that the data can be used in classic equations to predict flow rates at various pressures and coating thicknesses.

A geometry index "GI" was developed to normalize GM permeability values for coating thickness and cross-sectional area. The correlation between the UAB test and the normalized GM data does have a linear relationship (see Fig. 13). The thickness of the GM coating disc must be determined and recorded to correlate the two permeability values.

The normalized GM data were used to predict permeability under the same condition as the UAB procedure. The predicted flow rates were higher than the measured data, and the difference was greater for higher permeability coatings.

The literature on various gas flow regimes indicates that permeability measurements obtained using the GM procedure should be higher than measured because of gas compressibility and the mean free path slippage at low pressures. For a high permeability coating, the slippage increases because of the low test pressure. This contributes to the larger difference between the predicted results and measured data.

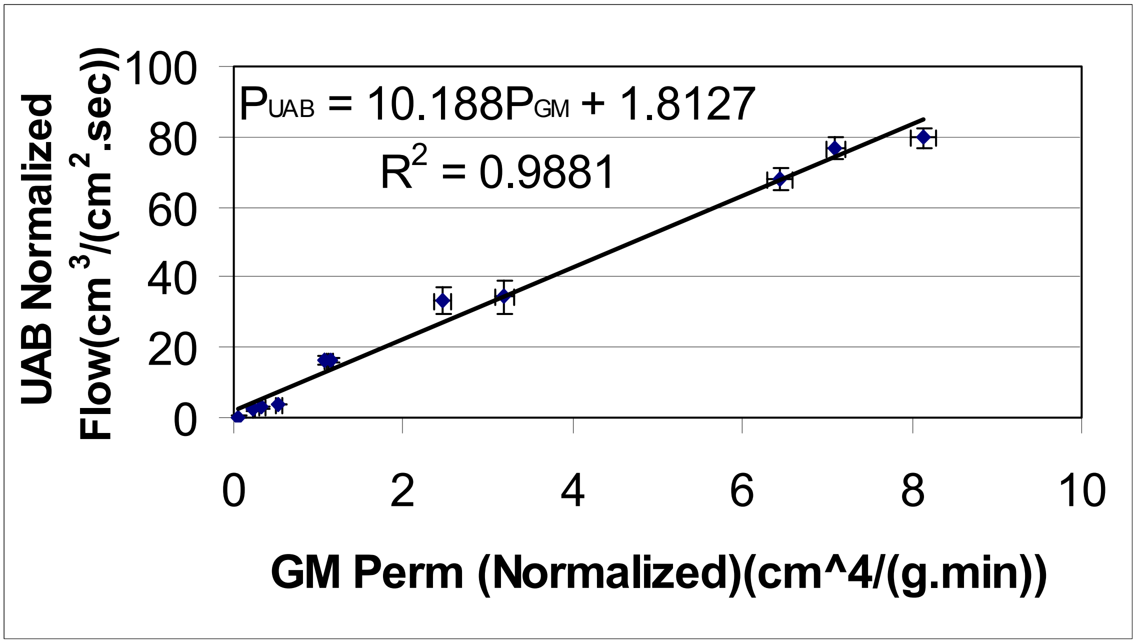

Fig. 13. Plot of Correlation between UAB and GM normalized Data. The normalized data fits a near perfect linear relationship.

5.1.3 Reorientation of Research Focus

Based on metal front shape and velocity measurements data obtained in x-ray studies of pouring GM plates, an effort was begun to evaluate effects of pattern open porosity on the ‘effective’ permeability of combined pattern/coating systems. Preliminary examinations indicated that the pattern open porosity made a significant contribution to the ‘effective’ system permeability. This may explain why previous research on modeling gas removal failed to balance the heat transfer and the gas removal equations. Based on above observations, additional research was conducted on pattern quality control procedures.

5.2 Coating Consistency

The goal of this study was to develop procedures to monitor pattern coating thickness. The Coating Quality Control Manual was revised and issued to participating companies. Current coatings are dramatically more consistent using these procedures.

5.3 Vacuum Assisted Pouring

The goal of this effort was to determine interactions between externally applied vacuum to assist in the removal of pattern pyrolysis products.

5.3.1 Drawback of Vacuum Assist

Earlier research indicated that pyrolysis products could be removed from the casting cavity using high vacuum levels. Unfortunately, the vacuum produced high metal flow rates and increased the incidence of defects including burned on sand and porosity.

5.3.2 Steel Casting

The goal of this investigation was to determine the feasibility of using the lost foam process to produce steel castings with a minimum of carbon pick-up.

With current pattern materials, this task is nearly impossible. All pattern materials pyrolize to produce carbon which is absorbed into the steel. Permission was given by the sponsors to discontinue work on this task. The effort was redirected to Task 6, In Plant Troubleshooting and Technology Exchange.

6. In-Plant Case Studies

The objective of this task was to assist sponsors solve in-plant problems associated with lost foam casting production. This process also helps UAB understand real production issues.

6.1 Case Study – Equipment Maintenance

A significant technology transfer effort occurred in an aluminum engine foundry. This foundry experienced high levels of scrap that was interrupting the flow of castings to the machining center. Process changes had been made without understanding the downstream effects, and equipment maintenance had been neglected. A process review found two areas in pattern production where significant improvements could be made. New procedures were implemented to measure bead density and to establish a time period for using the beads.

Procedures for measuring coating permeability and viscosity were implemented in both the foundry at the coating supplier. Within three months scrap rates had decreased from 40% to below 10%. A training seminar was then held to provide guidance for further improvements.

6.2 Case Study – Gas Cavity and Cold Laps in Iron Castings

Several experiments were conducted in an iron foundry to investigate the formation of a gas cavity in pipe flanges. SEM examination found that the defect was caused by entrapped pattern pyrolysis products. A group of foam patterns was wired with metal position probes and thermocouples (see Fig. 14) to understand the formation of the gas cavity defect. Metal filling profile, metal velocity and temperature near the flange were measured, and it was found that pipe sections did not fill evenly (see Fig. 15). It was also found that enlarging the bottom of the sprue decreased the filling time and produced more uniform filling.

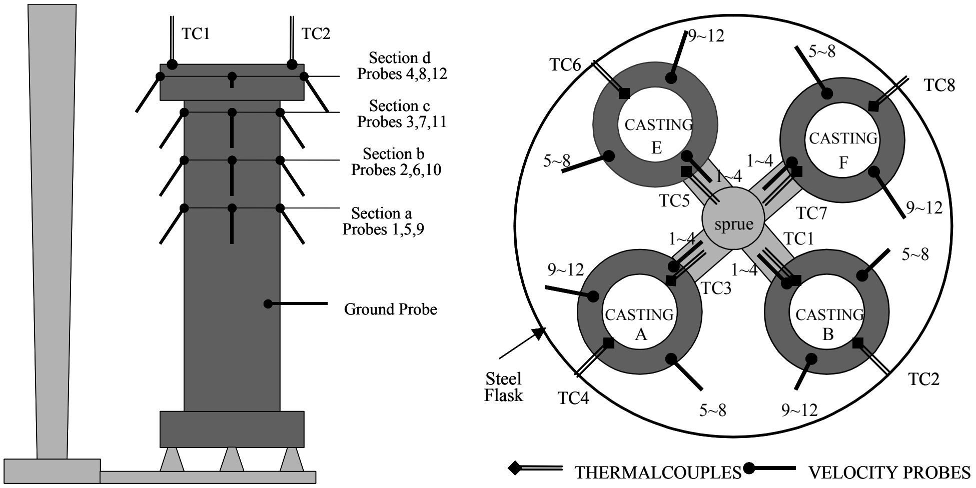
TC1
TC2
Section d
Probes 4,8,12
Section c
Probes 3,7,11
Section b
Probes 2,6,10
Section a
Probes 1,5,9
Ground Probe
9~12
5~8
TC6
TC8
CASTING E
CASTING F
5~8
1~4
1~4
9~12
TC5
sprue
TC7
1~4
TC1
9~12
1~4
5~8
TC3
CASTING A
CASTING B
Steel Flask
TC4
5~8
9~12
TC2
THERMALCOUPLES
VELOCITY PROBES

(a) (b)

Fig. 14. Location of metal position probes and thermocouples. Fifty-two position probes and eight pairs of thermocouples were inserted into foam pattern before cluster was put into flask: a) side view; b) top view.

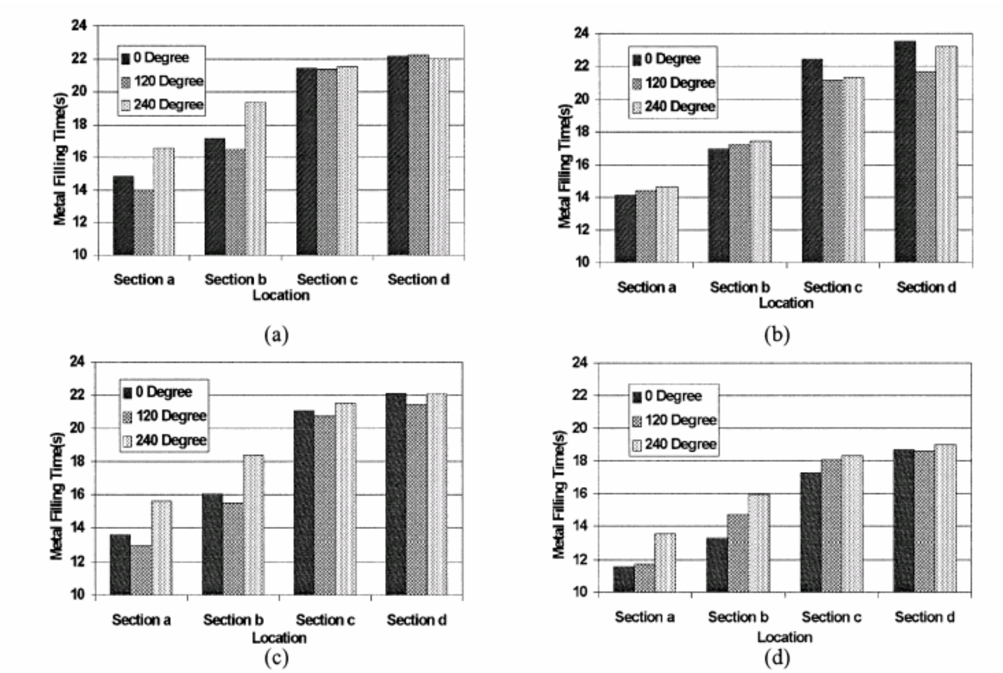

Fig. 15. Metal front profiles in different sections. Time that metal reached position probes is filling time. The longer the filling time, the lower the metal level is: a) casting A; b) casting B; c) casting E; d) casting F.

In addition to the gas cavity defect, surface defects (cold laps) were also experienced. Temperature measurements in the mold found that the metal was only slightly above the liquidus as the top flange was filled. Experiments were conducted to determine metal and sand temperatures. It was found that the defects could be eliminated by increasing the sand temperature by 25°F. The slightly elevated sand temperature provided time for liquid pyrolysis to escape and produce a smooth metal fill profile. The scrap total scrap rate fell to below 5%.

6.3 Case Study – Pattern Quality and Casting Quality

A ductile iron foundry experienced periods of high scrap rates associated with different batches of patterns. The 'good' batch produced castings with less than 5% scrap while the 'bad' batch produced 25% scrap. Pattern density and porosity measurements found that scrap was associated with high density and open porosity gradients even though the average pattern densities were identical.

The polymer molecular weight (Mw) and the glass transition temperature (Tg) were determined and no difference was found between either values in the 'good' and 'bad' batches of patterns. Other parameters including coating permeability and viscosity, and metal temperature were within normal limits. The density variations which were at the root of the problem were thought to be caused by the pattern blowing operation, but data could not be obtained from the pattern shop to prove it.

6.4 Case Study – Pattern Permeability Control on the Production Floor

Designed experiments were conducted at a sponsor foundry to determine the effect of pattern permeability on the occurrence of casting defects. The goal was to determine the effect of pattern permeability by blowing patterns having different pentane contents. It was found that:

1) Pentane contents from 1.7 % to 2.4 % resulted in a wide range of pattern permeabilities with the lower pentane levels producing the higher values.

2) Casting scrap decreased with increasing pentane contents and lower pattern permeabilities; and,

3) A large permeability range was found in pattern slices where porosity defects occurred. The permeability range was related to the location of fill guns.

Real time x-rays of a section of a cylinder head found that gas holes was originated from lighteners in a pattern slice. The tool was modified to eliminate the blind holes and the two fill guns added. The acceptable pentane at during blowing was changed, and scrap decreased to less than 3%.

6.5 Case Study – Shot Blast Carryover

Shot blasting materials were found to be the cause of casting defects in one plant. Steel shot were found using SEM and EDX analysis in the defect. These steel balls probably came from remelted parts that had been shot blasted.

6.6 Case study – Pore Defect in a Lost Foam Iron Casting

Experiments were conducted to identify causes of a pore defect. The casting sample was x-rayed and additional interior pores found. The casting was fractured and the surfaces were analyzed with SEM and EDX. Coating debris, as well as carbon was found. This indicates that the defect was caused by foam pyrolysis, but not by slag as thought. Experiments are underway to eliminate the problem.

7. Energy and Environmental Data

The available data from sponsors was received and reviewed. The most comprehensive report received was "Life Cycle Assessment of Aluminum Casting Processes" prepared by GM Corporation.

The Life Cycle report compares Lost Foam to other casting processes including semi-permanent mold and precision sand processes. The environmental burdens associated with raw material, energy consumption, gaseous emissions, and waste generation are analyzed. In general, the environmental burdens associated with the Lost Foam and semi-permanent mold processes were similar and lower than burdens associated with precision sand process. Overall, Lost Foam was determined to be the most environmentally friendly process.

8. Technology Transfer

The objective of this work was to assure timely and cost effective project performance, disseminate technical information to project participants, the U.S. metals casting industry, associated industries, and the general public.

Technology transfer between UAB personnel and sponsors occurs in the form of meetings at four month intervals and individual contact as requested by the sponsors. These meetings provide reviews of the research achievements and input from the sponsors concerning future directions.

Two levels of training courses have been prepared and used. These are referred to as (1) Entry level for new employees and (2) Process Understanding for Engineers and Key Production Personnel. These courses have increased the understanding of features that control the Lost Foam Process. The information has been presented to sponsors in seminars and the manuals distributed to sponsor companies. These courses were directed at process control personnel including supervisors, engineers, and managers. The important parameters controlling the process are presented along with measurement and data analysis procedures.

Follow-up visits to foundries have been encouraging. The increased understanding of the controlling features of the process has significantly increased the attention to details on the production floor.

The following are details of the sponsor meetings given in the past years:

No.	Meeting location and date	Participant man-hours
1	Chicago, IL on October 20 -21, 1999	756
2	Birmingham, AL on February 16-17, 2000	648
3	Chicago, IL on June 20 -21, 2000	568
4	Chicago, IL on October 17 -18, 2000	492
5	Birmingham, AL on February 16-17, 2001	540
6	Chicago, IL on June 20 -21, 2001	456
7	Saginaw, MI on Oct. 22, 2001	344
8	Birmingham, AL on February 19-20, 2002	432
9	Frankenmuth, MI on June 19-20, 2002	432
10	Saginaw, MI on Oct. 23-24, 2002	648
11	Birmingham, AL on February 19-20, 2003	548
12	Knoxville, TN on June 5, 2003	216
13	Chicago, IL on Oct. 23, 2003	256

Interaction with the sponsors at these meetings allows sponsors to respond to the project progress and provide direction for further research. Based on sponsor directions the research focus has generally dealt with (1) developing a computational models that describe mold filling and metal solidification, (2) reducing casting defects to metal properties and conserve energy, (3) improve casting accuracy and precision, and (4) determining environmental emissions.

A survey was conducted among sponsors in February 2003 to determine the areas of most interest. The results of the survey are presented below with higher rating numbers indicating high priority research topics.

Summary of Research Priorities as Established by Project Participants

Research Topic	Rating
A. Computational Model	98
B. Aluminum Defect Reduction	96
C. Aluminum Property Data	94
D. Pattern and Bead Variability	90
E. Improved Coatings	81
F. Alternate Pattern Materials	80
G. Casting Dimensions	73
H. Glue Related Defects	69
I. Iron Defect Reduction	62
J. Iron Property Data	56
K. Ductile Iron Property Data	54
L. Emissions	52
M. Low Volume Products	43

These priorities fall into five general categories including (1) development of a computational model that will describe mold filling and metal solidification (Item A), (2) reduced casting defects that will improve metal properties and conserve energy (Items B, C, D, E, F, H, I, J, K), (3) improved casting accuracy and precision (Item G), and (4) environmental emissions (Item L).

Results of the research are also presented at national and/or international conferences such as those held by the American Foundry Society and the Materials Society (TMS).

ACKNOWLEDGMENTS

We wish to express grateful acknowledgment and deep appreciation to the many companies and individuals who participated in the project by providing advice, descriptions of particular difficulties, defects, and guidance regarding the most fruitful areas for investigation.

A special word of thanks goes to Joe Santner for guidance throughout the project. We also wish to express our appreciation to the Department of Energy for technical assistance and partial funding of the project. Special thanks go to Bob Trimberger, Ehr Ping Huangfu and Dibyajyoti Aichbhaumik. Matching funds from DOE were provided under Cooperative Agreement DE-FC07-99ID13840 with Amendments. Matching funds were also provided to the University of Missouri at Rolla by the Missouri Research and Training Center.

Our hope is that the information contained in this report will be of assistance to companies throughout the United States in advancing the technology of Lost Foam Casting.

CHARLES E. BATES

HARRY E. LITTLETON

WANLIANG SUN

USE OF THIS REPORT AND INFORMATION CONTAINED THEREIN

Limitation of Liability

The faculty and staff of UAB associated with this project have used their professional experience and best professional efforts in performing this work. However, UAB DOEs not represent, warrant or guarantee that its research results, or product produced therefrom, are merchantable or satisfactory for any particular purpose, and there are no warranties, express or implied, to such effect. Acceptance, reliance on, or use of such results shall be at the sole risk of Sponsor. In connection with this work, UAB shall in no event be responsible or liable in contract or in tort for any special, indirect, incidental or consequential damages, such as, but not limited to, loss of product, profits or revenues, damage or loss from operation or nonoperation of plant, or claims of customers of Sponsor.

Report No.: 527985-2004 Project Final Report

To: Department of Energy; The American Foundry Society; and
the AFS/DOE/LFC Foam Casting Consortium Member Companies

Date: February 22, 2005